

**MECHANICAL PROPERTIES ENHANCEMENT OF HYDROGEL
USING NARROW DISPERSED MODIFIED SILICA PARTICLES
AS CROSS-LINKER**

BY

MD. REZAUL KARIM

STUDENT ID. 0417032708F

SESSION: APRIL 2017

MASTER OF SCIENCE IN CHEMISTRY



**Soft and Smart Materials Research Group
Department of Chemistry
Bangladesh University of Engineering and Technology
(BUET)**

August 2019

Bangladesh University of Engineering and Technology
Department of Chemistry




The thesis entitled 'MECHANICAL PROPERTIES ENHANCEMENT OF HYDROGEL USING NARROW DISPERSED MODIFIED SILICA PARTICLES AS CROSS-LINKER, submitted by MD. REZAUL KARIM, Roll No.: 0417032708F Session: April-2017, has been accepted as satisfactory in partial fulfillment of the requirement for the degree of Master of Science (M. Sc.) in Chemistry on 27.08.2019.

Board of examiners

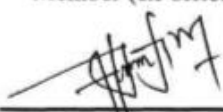
1. Dr. Abu Bin Imran
Associate professor
Department of chemistry
BUET, Dhaka.
(Supervisor)


Chairman

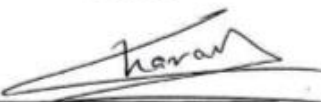
2. Head
Department of chemistry
BUET, Dhaka.


Member (ex-officio)


3. Dr. Md. Shakhawat Hossain Firoz
Professor
Department of chemistry
BUET, Dhaka.


Member

4. Dr. Chanchal Kumar Roy
Assistant Professor
Department of chemistry
BUET, Dhaka.


Member

5. Dr. Md. Mufazzal Hossain
Professor
Department of Chemistry
University of Dhaka, Dhaka-1000


Member (External)

Declaration by the candidate

I am hereby declared that this thesis or part of it has not been submitted elsewhere for award of any degree or diploma

.....
Md. Rezaul Karim
August 2019

**Dedicated to
My Beloved Parents
&
My Honorable Supervisor**

Acknowledgement

At the beginning, I humbly acknowledge my deepest gratitude to the almighty, the most gracious, benevolent and merciful creator for his infinite mercy bestowed on me in carrying out the research work presented in the dissertation. It is a great pleasure for me to acknowledge my deepest sense of gratitude, sincere appreciation, heartfelt indebtedness and solemn regards to my reverend teacher and supervisor Dr. Abu Bin Imran, Associate Professor, Department of Chemistry, Bangladesh University of Engineering and Technology (BUET), for his kind supervision, indispensable guidance, valuable and constructive suggestions, liberal help and continuous encouragement during the whole period. It is obvious that his attributive contribution and efforts have greatly shaped me into what I am today. In fact, I am quite lucky to be a part of his ambitious research team. It is my great honor to convey my sincere gratitude to my respected teacher Professor Dr. Md. Abdur Rashid Honorable Head, Department of Chemistry, BUET for giving me his wonderful support to move through the academic processes during this M.Sc. program. I would like to convey my deepest gratitude to Professor Dr. Md. Shakhawat Hossain Firoz, Dr. Chanchal Kumar Roy of the Department of Chemistry, BUET and Dr. Md. Mufazzal Hossain, Department of Chemistry, University of Dhaka for their valuable suggestions, appreciated comments, guidance and help during the research period. I am thankful to all other respected teachers of the Department of Chemistry, BUET, for their continuous support. I would also like to thank all of the officers and staffs of the Department of Chemistry, BUET for their relentless help during my study period. I am grateful to Department of Glass and Ceramics Engineering, Bangladesh University of Engineering and Technology for the sample characterizations of FE-SEM and EDX during my research. I am highly grateful to all members of the board of examiners for their valuable suggestions and appreciated comments. I am thankful to my dear consociate and all the members of Soft and Smart Materials Research Group for their friendly cooperation and lovely encouragement throughout my research period. My special thanks to Solaiman, Noman Chowdhury, Tarun Kante Majumder, Md. Aminur Rahman, H. B. Muhammad Zukaul Islam, Sarmin Akter, Md. Amjad Hossain, and Md. Mosfeq Uddin for their continuous help during the research. Finally, I would like to express my heartfelt indebtedness and profound gratitude to my beloved father, mother and all of my family members for their continuous inspiration and

immeasurable sacrifices throughout the period of my study.

Md. Rezaul Karim

August 2019

Abstract

Hydrogels are widely used in manifold applications but the scope of their applications is often severely limited by their poor mechanical behaviors including low toughness and limited stretchability. Many attempts are carried out together to synthesize hydrogels with improved mechanical properties. However, yet to achieve the facile and universal approach to fabricate hydrogel with desired strength and biocompatibility. Here, we have successfully developed hydrogels with high tensile strength and toughness by reinforcing the network structure of acrylamide with grafted silica nanoparticles as cross-linker. Silica nanoparticles grafted with vinyl end groups using 3-(trimethoxysilyl)propyl methacrylate (MPTS) was used as macro-crosslinker during polymerization reaction of acrylamide in presence of modified silica (MSiO_2) to form nanocomposite hydrogel. Three kinds of silica particle with different particle sizes 100nm, 200nm and 300nm were used to prepare MSiO_2 . The unique nature of synthesized nanocomposite hydrogel which contains both organic and inorganic substances led to their wide-spread applications as they have remarkable stretching, and toughness of $\sim 59,400 \text{ J m}^{-2}$ for the elongation. In addition, all the synthesized hydrogels showed high transparency (above 75%) in the wavelengths of visible region light. The tensile test of stress-strain measurements of 100 nm silica containing hydrogels significantly increased the mechanical performance compare with the other 200 nm, 300 nm silica containing hydrogel. In contrast, the compressive stress-strain measurements did not show any significant change. The polymer chains inside the nanocomposite hydrogel can dissipate energy during applied stress while the chemical cross-links between MSiO_2 and polyacrylamide ensure the structural integrity, which could be responsible for the improved mechanical properties of fabricated nanocomposite hydrogel.

Contents

Acknowledgement	v
Abstract	vii
Contents	viii
List of figures	xii
List of tables	xiv
List of Abbreviations of Technical Symbols and Terms	xvi
Chapter 1 Introduction	1
1.1 Hydrogels.....	3
1.2 Classification of hydrogels	3
<i>1.2.1 Classification based on cross-linking</i>	3
<i>1.2.1.1 Physically cross-linked hydrogels</i>	4
<i>1.2.1.1.1 Ionic interaction</i>	4
<i>1.2.1.1.2 H-bonding</i>	4
<i>1.2.1.1.3 Stereo complex formation</i>	5
<i>1.2.1.1.4 Freeze-thawing</i>	5
<i>1.2.1.2 Chemically cross-linked hydrogels</i>	5
<i>1.2.1.2.1 Chemical cross-linking</i>	5
<i>1.2.1.2.2 Grafting</i>	5
<i>1.2.1.2.2.1 Chemical grafting</i>	5
<i>1.2.1.2.2.2 Radiation grafting</i>	5
<i>1.2.1.2.3 Radical polymerization</i>	6
<i>1.2.1.2.4 Condensation reaction</i>	6
1.3 Effect of crosslinking.....	6
<i>1.3.1 Elasticity</i>	6

1.3.2 Decrease in the viscosity.....	7
1.3.3 Insolubility of the polymer	7
1.3.4 Increased T_g	7
1.3.5 Lower melting point.....	7
1.3.6 Transformation of thermoplasts into thermosets	8
1.4 Methods of preparation.....	8
1.4.1 Homo-polymeric hydrogels.....	8
1.4.2 Co-polymeric hydrogels.....	8
1.4.3 Semi-interpenetrating network (semi-IPN).....	8
1.4.4 Stimuli responsive hydrogel.....	9
1.4.4.1 pH responsive hydrogels.....	10
1.4.4.2 Thermoresponsive hydrogels	10
1.5 Properties of hydrogel.....	11
1.5.1 Mechanical property.....	11
1.5.1.1 Tensile strength.....	12
1.5.1.2 Young's Modulus.....	13
1.5.1.3 Ductility	13
1.5.1.3 Toughness	13
1.5.1.4 Mechanically strong hydrogel	14
1.5.1.4.1 Topological hydrogel.....	14
1.5.1.4.2 Double-network hydrogels (DN gels).....	14
1.5.1.4.3 Macromolecular microsphere (MMC) hydrogels.....	14
1.5.1.4.4 Nanocomposite hydrogel (NC gels).....	15
1.5.2 Biocompatible properties.....	15
1.5.3 Swelling Properties.....	16
1.6 Application of Hydrogel	17
1.6.1 Drug delivery applications	17
1.6.2 Hydrogel in agriculture	17
1.7 Literature Review	18
1.8 Research Goal	19

1.9 References.....	20
Chapter 2 Experimental.....	29
2.1. Materials and instruments.....	24
2.1.1. Chemicals.....	24
2.1.2. Instrument.....	25
2.2. Method of preparation.....	25
2.2.1. Preparation of modified silica particles (MSiO ₂).....	25
2.2.2.(i) Schematic diagram for preparation of MSiO ₂	26
2.2.2.(ii) General preparation scheme of MSiO ₂	27
2.2.3. Preparation of MSiO ₂ nanocomposite hydrogels.....	27
2.2.4. Preparation recipe of different hydrogels.....	28
2.3 Characterizations.....	30
2.3.1. Fourier transform infrared (FTIR) spectroscopy analysis.....	30
2.3.2. Nuclear magnetic resonance (NMR) analysis.....	30
2.3.3. Field emission scanning electron microscopy (FE-SEM).....	30
2.3.4. Energy dispersive x-ray spectroscopy (EDS).....	30
2.3.5. Mechanical properties analysis for elongation.....	31
2.3.6 The compressive stress–strain measurements.....	31
2.3.7 Transmittance spectra.....	31
2.4 References.....	33
Chapter 3 Results and Discussion.....	34
3.1 Synthesis of AAm-MSiO ₂ nanocomposite hydrogel.....	35
3.2 Mechanism of free radical polymerization of AAm.....	36
3.2.1 Proposed chemical structure of AAm-MSiO ₂ hydrogel.....	37
3.3 Functional Group investigation by Fourier Transform Infrared (FT-IR) Spectroscopy.....	37
3.4 Study of surface morphology SiO ₂ (300nm) and MSiO ₂ (300nm).....	40
3.5 Study of surface morphology SiO ₂ (200nm) and MSiO ₂ (200nm).....	41
3.6. Study of surface morphology MSiO ₂ (100nm).....	42

3.7 EDS analysis of MSiO ₂ (300 nm).....	43
3.8 EDS analysis of SiO ₂ (200 nm)	44
3.9 EDS analysis of MSiO ₂ (200 nm).....	45
3.10 EDS spectra of MSiO ₂ (100 nm)	46
3.11 Transmittance spectra of synthesized hydrogels	47
3.12.1 Tensile test of AAm -BIS hydrogels.....	47
3.12.2 Comparison of tensile test of AAm-MSiO ₂ (216.5 nm) and AAm-BIS hydrogels..	49
3.12.3 Compressive strength of AAm -BIS hydrogels.....	50
3.12.4 Comparison of compressive strength of AAm-BIS and AAm-MSiO ₂ hydrogels..	52
3.12.5 Tensile test of AAm-MSiO ₂ -BIS (A ₂ S _{Y%B.7}) hydrogels.....	53
3.12.6 Tensile test of AAm -MSiO ₂ (216.5 nm) hydrogels with varying concentration MSiO ₂	54
3.12.7 Compressive strength of AAm-MSiO ₂ (216.5 nm) hydrogels prepared by varying concentration of MSiO ₂	56
3.12.8 Tensile test of different AAm-MSiO ₂ ((117.5 nm, 216.5 nm and 311.5 nm) hydrogels prepared by varying concentration of AAm	57
3.12.9 Compressive strength of AAm-MSiO ₂ hydrogels (117.5 nm, 216.5 nm and 311.5 nm) prepared by varying concentration of AAm.....	59
3.12.10 Comparison of tensile test of AAm-MSiO ₂ hydrogels prepared by varying particle sizes of MSiO ₂ (117.5 nm, 216.5 nm,311.5 nm)	62
3.12.11 Comparison of compressive strength of AAm-MSiO ₂ hydrogels prepared by varying particle sizes of MSiO ₂ (117.5 nm, 216.5 nm,311.5 nm).....	66
3.13 Photographs of AAm-MSiO ₂ hydrogel during analysis of stress-strain curves under uniaxial tensile deformation	71
3.14: Photographs of AAm-MSiO ₂ hydrogel during analysis of stress-strain curves under uniaxial compressive deformation	72
3.15. References.....	73
Chapter 4 Conclusion	74
4. Conclusion	75
Publication, Attended conference and Achievement	76

List of figures

Fig. 1. 1: Photograph of as prepared hydrogel.....	3
Fig. 1. 2 Physical cross-linked hydrogel.....	4
Fig. 1. 3:Chemically cross-linked hydrogel.....	5
Fig. 1. 4: Schematic illustration of a hydrogel that can undergo reversible volume phase transitions upon minute changes in environmental condition	10
Fig. 1. 5: pH responsive hydrogel.....	10
Fig. 1. 6: Positive and negative temperature responsive hydrogels.....	11
Fig. 1. 7: Stress- strain curve	12
Fig. 1. 8 : Ductility test of a material	13
Fig. 1. 9: Drug released from hydrogel.....	17
Fig. 1. 10 : Hydrogel in agriculture	18
Fig. 2. 1:Synthesis route of modified silica (MSiO ₂)	27
Fig. 3. 1: AAm-MSiO ₂ nanocomposite hydrogel	35
Fig. 3. 2: FT-IR spectra of bare SiO ₂ and MSiO ₂	38
Fig. 3. 3: ¹ H-NMR spectra of bare SiO ₂	39
Fig. 3. 4: ¹ H-NMR spectra of MSiO ₂	39
Fig. 3. 5 : SEM image of a) bare SiO ₂ (300 nm) with magnification×50,000 and b) MSiO ₂ (300 nm) with magnification ×50,000.....	41
Fig. 3. 6 : Particle size distribution curve of Silica(302.5 nm) and MSiO ₂ (311.5nm) using imageJ software	41
Fig. 3. 7 : SEM image of a) bare SiO ₂ (200nm) with magnification×100,000 and b) MSiO ₂ (200 nm) with magnification ×100,000	42
Fig. 3. 8 : Particle size distribution curve of SiO ₂ (208.5 nm) and MSiO ₂ using imageJ software	42
Fig. 3. 9 : SEM image for a) MSiO ₂ (100 nm) with magnification×100,000 and b) magnification ×50,000.....	43
Fig. 3. 10 : Particle size distribution curve of MSiO ₂ (117.5 nm) using imageJ software	43
Fig. 3. 11: EDS spectra of MSiO ₂ (300nm).....	44
Fig. 3. 12: EDS spectra of bare SiO ₂ (200nm).....	45
Fig. 3. 13: EDS spectra of MSiO ₂ (200nm).....	45

Fig. 3. 14: EDS spectra of MSiO ₂ (100nm).....	46
Fig. 3. 15: Transmittance spectra of AAm-MSiO ₂ hydrogels	47
Fig. 3. 16: Photograph of highly transparent AAm-MSiO ₂ hydrogels	47
Fig. 3.17:Stress –strain curves of AAm-BIS hydrogels prepared by varying concentration of BIS under uniaxial tension	48
Fig. 3. 18:Stress –strain curves of AAm-MSiO ₂ and AAm-BIS hydrogels prepared by varying concentration of BIS and MSiO ₂ under uniaxial tension.	50
Fig. 3. 19: Stress –strain curves of AAm-BIS hydrogels prepared by varying concentration of BIS under uniaxial compression.	51
Fig. 3.20: Stress –strain curves of AAm-MSiO ₂ and AAm-BIS hydrogels prepared by varying concentration of BIS and MSiO ₂ under uniaxial compression.	52
Fig. 3. 21: Stress –strain curves of AAm-MSiO ₂ -BIS hydrogels prepared by varying concentration of BIS and MSiO ₂ under uniaxial tension.	53
Fig. 3. 22 : Stress –strain curves of AAm-MSiO ₂ (216.5 nm) hydrogels prepared by varying concentration of MSiO ₂ under uniaxial compression.	56
Fig. 3. 23: Stress –strain curves of AAm-MSiO ₂ (216.5 nm) hydrogels prepared by varying concentration of AAm under uniaxial tension.	58
Fig. 3. 24 : Stress –strain curves of AAm-MSiO ₂ (311.5 nm) hydrogels prepared by varying concentration of AAm under uniaxial tension.	59
Fig. 3. 25 : Stress –strain curves of AAm-MSiO ₂ (117.5 nm) hydrogels prepared by varying concentration of AAm under uniaxial compression.....	60
Fig. 3. 26 : Stress –strain curves of AAm-MSiO ₂ (216.5 nm) hydrogels prepared by varying concentration of AAm under uniaxial compression.....	61
Fig. 3. 27 : Stress –strain curves of AAm-MSiO ₂ (311.5 nm) hydrogels prepared by varying concentration of AAm under uniaxial compression.....	62
Fig. 3. 28 : Stress –strain curves of AAm-MSiO ₂ hydrogels prepared by varying particle sizes of MSiO ₂ (117.5 nm, 216.5 nm,311.5 nm) but AAm concentration kept constant as 4M under uniaxial tension.....	64
Fig. 3. 29 : Stress –strain curves of AAm-MSiO ₂ hydrogels prepared by varying particle sizes of MSiO ₂ (117.5 nm, 216.5 nm,311.5 nm) but AAm concentration kept constant as 5M under uniaxial tension.....	65
Fig. 3. 30 :Tensile strength of AAm-MSiO ₂ hydrogel with different concentration of AAm for elongation	66
Fig. 3. 31 :Toughness and young's modulus of AAm-MSiO ₂ hydrogel with	

different concentration of AAm for elongation.....	66
Fig. 3. 32 : Stress –strain curves of AAm-MSiO ₂ hydrogels prepared by varying particle sizes of MSiO ₂ (117.5nm, 216.5nm,311.5nm) but AAm concentration kept constant as 3M under uniaxial compression.....	67
Fig. 3. 33 : Stress –strain curves of AAm-MSiO ₂ hydrogels prepared by varying particle sizes of MSiO ₂ (117.5nm, 216.5nm,311.5nm) but AAm concentration kept constant as 4M under uniaxial compression.....	68
Fig. 3. 34 : Stress –strain curves of AAm-MSiO ₂ hydrogels prepared by varying particle sizes of MSiO ₂ (117.5nm, 216.5nm,311.5nm) but AAm concentration kept constant as 5M under uniaxial compression.....	69
Fig. 3. 35: Compressive strength of AAm-MSiO ₂ hydrogel with different concentration of AAm	70
Fig. 3. 36: Toughness and young’s modulus of AAm-MSiO ₂ hydrogel during compression in different concentration of AAm	70
Fig. 3. 37: Photographs of AAm-MSiO ₂ hydrogel during analysis of stress-strain curves under uniaxial tension	71
Fig. 3. 38: Photographs of AAm-MSiO ₂ hydrogel during analysis of stress-strain curves under uniaxial compressive deformations	72

List of tables

Table 2. 1: Preparation recipe of AAm-BIS hydrogels.....	28
Table 2. 2: Preparation recipe of AAm-BIS- MSiO ₂ hydrogels	28
Table 2. 3: Preparation recipe of AAm-MSiO ₂ hydrogel	29
Table 2. 4 : Preparation recipe of AAm-MSiO ₂ hydrogel for different silica.....	29
Table 3. 1: Characteristic peaks of SiO ₂ and MSiO ₂	38
Table 3. 2: ¹ H-NMR data for MSiO ₂	40
Table 3. 3: EDS spectra of MSiO ₂ (300 nm)	44
Table 3. 4 : EDS spectra of bare SiO ₂ (200 nm).....	45
Table 3. 5: EDS spectra of MSiO ₂ (200 nm)	46
Table 3. 6: EDS spectra of MSiO ₂ (100 nm)	46
Table 3. 7: Table for tensile properties of AAm-BIS hydrogels prepared by varying concentration of BIS	49
Table 3. 8 : Tensile properties of AAm-MSiO ₂ and AAm-BIS hydrogels.....	50

Table 3. 9 :Table for compressive properties of AAm-BIS hydrogels prepared by varying concentration of BIS	51
Table 3. 10 :Compressive strength of AAm-MSiO ₂ and AAm-BIS hydrogels prepared by varying concentration of BIS and MSiO ₂	52
Table 3. 11 : Table for tensile properties of AAm-MSiO ₂ -BIS (A ₂ S _Y B. ₇) hydrogels.....	54
Table 3. 12 : Table for tensile properties of AAm-MSiO ₂ (216.5 nm) hydrogels prepared by varying concentration of MSiO ₂	55
Table 3. 13: Compressive properties of AAm-MSiO ₂ (216.5 nm) hydrogels prepared by varying concentration of MSiO ₂	56
Table 3. 14 :Table for tensile properties of AAm-MSiO ₂ (117.5 nm) hydrogels prepared by varying concentration of AAm.....	58
Table 3. 15: Table for tensile properties of AAm-MSiO ₂ (216.5 nm) hydrogels prepared by varying concentration of AAm.....	58
Table 3.16: Table for tensile properties of AAm-MSiO ₂ (311.5 nm) hydrogels prepared by varying concentration of AAm.....	59
Table 3.17: Table for compressive properties of AAm-MSiO ₂ (117.5 nm) hydrogels prepared by varying concentration of AAm	60
Table 3.18: Table for compressive properties of AAm-MSiO ₂ (216.5 nm) hydrogels prepared by varying concentration of AAm	61
Table 3.19: Table for compressive properties of AAm-MSiO ₂ (311.5 nm) hydrogels prepared by varying concentration of AAm	62
Table 3. 20: Table for tensile properties of AAm-MSiO ₂ hydrogels prepared by varying particle sizes of MSiO ₂ (117.5 nm, 216.5 nm,311.5 nm) but AAm concentration kept constant as 3M	63
Table 3. 21:Table for tensile properties of AAm-MSiO ₂ hydrogels prepared by varying particle sizes of MSiO ₂ (117.5 nm, 216.5 nm,311.5 nm) but AAm concentration kept constant as 4M	64
Table 3. 22: Table for tensile properties of AAm-MSiO ₂ hydrogels prepared by varying particle sizes of MSiO ₂ (117.5 nm, 216.5 nm,311.5 nm) but AAm concentration kept constant as 5M	65
Table 3. 23: Table for compressive properties of AAm-MSiO ₂ hydrogels prepared by varying particle sizes of MSiO ₂ (117.5 nm, 216.5 nm,311.5 nm) but AAm concentration kept constant as 3M	67
Table 3. 24 :Table for compressive properties of AAm-MSiO ₂ hydrogels	

prepared by varying particle sizes of MSiO ₂ (117.5 nm, 216.5 nm,311.5 nm) but AAm concentration kept constant as 4M.....	68
Table 3. 25 : Table for compressive properties of AAm-MSiO ₂ hydrogels prepared by varying particle sizes of MSiO ₂ (117.5 nm, 216.5 nm,311.5 nm) but AAm concentration kept constant as 5M.....	69

List of Abbreviations of Technical Symbols and Terms

1. Acrylamide (AAm)
2. 3-(Trimethoxysilyl)propyl methacrylate (MPTS)
3. Nanocomposite hydrogel (NC gels)
4. Modified silica (MSiO₂)
5. Polyacrylamide- MSiO₂ hydrogel (AAm-MSiO₂)
6. Poly(vinyl alcohol) (PVA)
7. Poly *N*-isopropyl acrylamide (PNIPAAm)

Chapter 1

Introduction

1.1 Hydrogels

Hydrogels are three-dimensional (3D) network of hydrophilic polymer chains that can swell in water and hold a large amount of water and possess solids and liquids like properties [1]. It maintains the structure due to the chemical or physical cross-linking of individual polymer chains [2]. Hydrogels were first reported by Wichterle and Lím (1960) [3]. By definition, water must constitute at least 10% of the total weight (or volume) for a material to be a hydrogel [4]. Hydrogels also possess a degree of flexibility very similar to natural tissue due to their significant water content. The hydrophilicity of the polymer network is due to the presence of hydrophilic groups such as $-NH_2$, $-COOH$, $-OH$, $-CONH_2$, $-CONH-$, and $-SO_3H$ [5- 7]. A variety of crosslinkers namely *N, N*-methylenebisacrylamide (BIS), *N, N*-cystaminebisacrylamide (CBA), 1,4-butanediol diacrylate (BDDA) are used for this purpose [8]. They have widely been used in many fields such as drug delivery systems, sensors, actuators, biomaterials and so on. But the potential applications of the hydrogel are often limited by their poor mechanical performances, for example too weak or brittle in nature, low toughness, low stretching and bending ability, low elastic modulus, etc. [9-10]. To overcome these limitations some attempts, have already been made. A pictorial representation of a hydrogel is shown in the following fig.1.1.



Fig. 1. 1: Photograph of as prepared hydrogel

1.2 Classification of hydrogels

The hydrogels can be classified in different ways as discussed below

1.2.1 Classification based on cross-linking

Based on cross-linking hydrogels are classified into two categories: (a) physically cross-linked hydrogel and (b) chemically cross-linked hydrogel [11-12]. Various types of chemical and physical crosslinking hydrogels were prepared with natural/synthetic polymers and used in miscellaneous applications.

1.2.1.1 Physically cross-linked hydrogels

Physically crosslinked hydrogels are developed by ionic interaction, crystallization, stereo complex formation, hydrophobized polysaccharides, protein interaction and hydrogen bond [13]. Physically cross-linked hydrogels have gained significant attention due to their relative ease of production and the advantage of not using cross-linking agents during their synthesis protocol [14]. The dissolution of physically cross-linked gels is prevented by physical interactions, which exist between different polymer chains. The various methods reported for obtaining physically cross-linked hydrogels are discussed below.

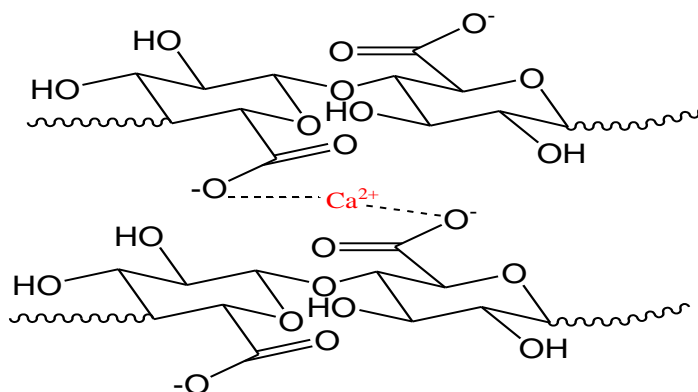


Fig. 1. 2 Physical cross-linked hydrogel

1.2.1.1.1 Ionic interaction

Ionic polymers cross-linked by the addition of di- or tri-valent counter ions in hydrogel systems falls in this category. This method underlies the principle of gelling a polyelectrolyte solution with multivalent ions of opposite charge [15]. Examples of the hydrogels that belong to this category are chitosan-glycerol phosphate salt and poly-[di(carboxylatophenoxy) phosphazene calcium salt.

1.2.1.1.2 H-bonding

Physically cross-linked gel-like structures can be prepared via hydrogen bonding interactions. The best example of such hydrogel is the formation of hydrogen-bond carboxymethylcellulose (CMC) network by dispersing CMC in 0.1 M HCl [16]. In this process, the sodium ions are replaced in CMC by hydrogen of the acid.

1.2.1.1.3 Stereo complex formation

In recent years, hydrogels have been generated for drug delivery systems that are based on stereo complex formation. The major advantage of this system is that a hydrogel can be easily formed by dissolving each product in water and mixing the solution. One best example that exhibits good stereo complex properties is PLA. The ability of PLA to form stereo complexes was first described by Tsuji et al [17]. However, in the stereo complexation, relatively restricted range of polymer compositions are used that limit the process.

1.2.1.1.4 Freeze-thawing

Physical cross-linking can be achieved using repetitive freeze-thaw cycles. This mechanism involves the formation of microcrystals in the structure due to freezing and thawing. Poly (vinyl alcohol) (PVA) hydrogels prepared by freeze-thawing is a popular example [18]. These hydrogels are inter-connected by hydrogen bonding, exhibit more porosity, spongy, rubbery and higher elastic properties than PVA hydrogels fabricated by other methods.

1.2.1.2 Chemically cross-linked hydrogels

In chemically cross-linked hydrogels, covalent bonds exist between different polymer chains. Therefore, they are stable and cannot be dissolved in any solvents unless the covalent crosslink points are cleaved. The design flexibility of a physically cross-linked hydrogel is restricted, due to the difficulty in decoupling the variables, such as gelation time, internal network pore size, chemical functionalization and degradation time [19]. In contrast, chemical cross-linking results in a network with a relatively high mechanical strength and depending on the type of the chemical bonds in the building blocks and the crosslinks. The various methods reported in the literature for obtaining chemically cross-linked hydrogels are appended below.

1.2.1.2.1 Chemical cross-linking

In chemical cross-linked hydrogels, cross-linkers, such as: glutaraldehyde,

epichlorohydrin, adipic acid dihydrazide, and polyaldehydes, etc., are widely used to obtain cross-linked hydrogel networks of various synthetic and natural polymers [20]. Further, covalent linkages between polymer chains can be established by the reaction of functional groups, such as an amine-carboxylic acid or an isocyanate-OH/NH₂ reaction, or by Schiff base formation, with complementary reactivity [21]. Hydrogel composites, based on xanthan and PVA are cross-linked with epichlorohydrin.

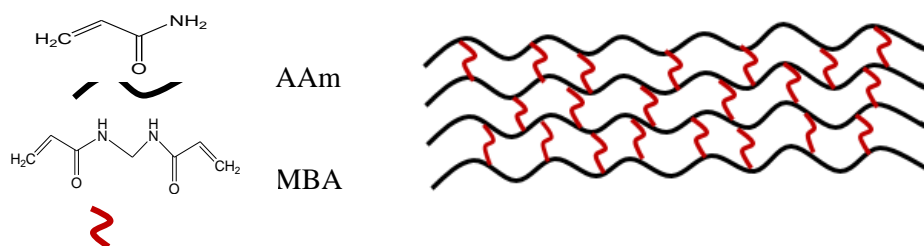


Fig. 1. 3:Chemically cross-linked hydrogel

1.2.1.2.2 Grafting

The preparation of hydrogels, based on grafting, involves the polymerization of a monomer on the backbone of a preformed polymer. Depending on the type of activation initiator, grafting can be classified as chemical grafting or radiation grafting.

1.2.1.2.2.1 Chemical grafting

In chemical grafting, macromolecular backbones are activated by the reaction of a chemical reagent. Grafting of acrylic acid (AA) onto granular maize starch in aqueous medium initiated by the ceric ion is an example of this system [22].

1.2.1.2.2.2 Radiation grafting

Grafting initiated by the use of high energy radiation, such as gamma and electron beam, is named as radiation grafting. Grafting of CMC with acrylic acid in presence of electron beam irradiation, in aqueous solution, is an example of radiation grafting [23]. The electron beam is used to initiate the free-radical polymerization of acrylic acid on the backbone of CMC.

1.2.1.2.3 Radical polymerization

Chemically cross-linked gels can also be obtained from low-molecular-weight monomers in the presence of a cross-linking agent by radical polymerization. This is one of the most widely used methods for the preparation of hydrogels. This is a very efficient system that results in the rapid formation of the gel, even under mild conditions. An example of this system is hydrogel fabrication from the free radical initiator: ammonium persulfate (APS) or potassium persulfate (KPS) [24-26].

1.2.1.2.4 Condensation reaction

Hydrogels formed through condensation reactions belong to this category. In general, the hydrogels involving hydroxyl groups/amines with carboxylic acids or their derivatives are used for the preparation of this type of hydrogels. The best example of these condensation reactions was described by De Nooy et al [27-28]. via the Passerini and Ugi condensation reactions. This Passerini condensation yields hydrogels with ester bonds in their crosslinks. In this typical process, carboxylic acid and the carbonyl compound (aldehyde or ketone) are condensed with an isocyanide, in order to yield α -(acryloxy) amide. In the Ugi condensation procedure, an amine is added to this reaction mixture, finally yielding α -(acrylamino) amide. The hydrogel of this type typically contains amide bonds in their crosslinks.

1.3 Effect of crosslinking

Adding cross-links between polymer chains affect the physical properties of the polymer depending upon the degree of cross linking and presence and absence of crystallinity. For example:

1.3.1 Elasticity

Elastomers are elastic polymers created by limited cross-linking. As the number of cross-links increases, however, the polymer becomes more rigid and cannot stretch as much; the polymer will become less viscous and less elastic and might even become

brittle. The vulcanization or sulfur curing of rubber, for example, results from the introduction of short chains of sulfur atoms that link the polymer chains in natural rubber. Bridges made by short chains of sulfur atoms tie one chain of polyisoprene to another, until all the chains are joined into one giant super molecule. The chemical process of vulcanization is a type of cross-linking which increases the strength of rubber [29]. It makes rubber hard and durable material associated with car and bike tires.

1.3.2 Decrease in the viscosity

In order for polymers to flow, the chains must move past each other and cross-linking prevents this [30]. As a result of restriction in flow there is improvement in the creep behavior.

1.3.3 Insolubility of the polymer

Cross-linking results in insolubility as the chains are tied together by a strong covalent bond. Crosslinked materials can't dissolve in solvents, but can absorb huge amount of water to form a gel. For example, cross-linked polyacrylamide gel. Uncross linked polyacrylamide is soluble in water, and crosslinked polyacrylamides can absorb water but are insoluble [31]. Water-logged gels of crosslinked polyacrylamides are used to make soft contact lenses [32].

1.3.4 Increased T_g

Crosslinking changes the local molecular packing, resulting in decrease in free volume, leading to an increase in T_g . PVA cross-linked with boric acid shows increased glass transition temperature [33]. Cross-links slow down the PVA molecular motion.

1.3.5 Lower melting point

For crystalline polymer with a low degree of cross-linking, there is a decrease in the crystalline behavior, as cross-linking introduces hindrance to the chain orientation resulting in a softer, elastic polymer having a lower melting point [34]

1.3.6 Transformation of thermoplasts into thermosets

Heavy cross-linking changes thermoplasts to thermoset plastics. Once the cross-links form, the polymer's shape cannot be changed again without destroying the plastic. Unlike thermoplastic polymers, the process cannot be undone by reheating; thermoset plastics will start to decompose rather than becoming moldable and pliable. The first thermoset was polyisoprene. More the sulfur crosslinks put into the polyisoprene, the stiffer it gets. Lightly crosslinked, it's flexible rubber. Heavily crosslinked becomes a hard thermoset [35].

1.4 Methods of preparation

The method of preparation leads to formation of some important classes of hydrogels. These can be exemplified by the following sections.

1.4.1 Homo-polymeric hydrogels

Homo-polymeric hydrogels are referred to as a polymer network derived from a single type of monomer which is a basic structural unit of any polymer network. Homopolymers may have cross-linked skeletal structure depending on the nature of the monomer and polymerization technique.

1.4.2 Co-polymeric hydrogels

Co-polymeric hydrogels are comprised of two or more different monomer types with at least one hydrophilic component arranged in a random, block or alternating configuration along the chain of the polymer network [36]. This co-polymer block is capable of forming a hydrogel when it is applied *in-situ*.

1.4.3 Semi-interpenetrating network (semi-IPN)

If one polymer is linear and penetrates another cross-linked network without any other

chemical bonds between them, it is called a semi-inter penetrating network [37]. It can more effectively exhibit rapid kinetic response rates with the change of pH or temperature.

1.4.4 Stimuli responsive hydrogel

Stimuli-responsive hydrogels represent a broad class of hydrogels undergoing switchable gel-to-solution or gel-to-solid transitions upon application of external triggers. Different physical or chemical external stimuli can be applied to induce reversible or single-cycle phase transitions of the hydrogels. These include thermal, magnetic, ultrasonic, electrochemical, or light stimuli as physical triggers, and pH, redox reactions, supramolecular complexes, and catalytically driven reactions as chemical triggers [38-39]. Numerous applications of stimuli-responsive hydrogels are suggested, including their use as functional matrices for sensing, actuators, and biomedical applications, such as controlled drug release, tissue engineering, and imaging [40]. Stimuli-triggered hydrogels are also used to construct catalytic switches, logic-gate operations, surfaces for the controlled growth of cells, and more. Methods to immobilize and pattern stimuli-responsive hydrogels on surfaces are developed, and the fabrication of surfaces revealing signal triggered stiffness and switchable interfacial electron transfer properties are reported. The synthetic advances in preparing nanometer- and micrometer-sized inorganic particles enable the incorporation of the micro- or nanoparticles into stimuli-responsive hydrogels to yield hybrid materials for electronic and optical applications. Additionally, methods to prepare stimuli-responsive nano-or micro hydrogels introduced new concepts for controlled and targeted drug release [41].

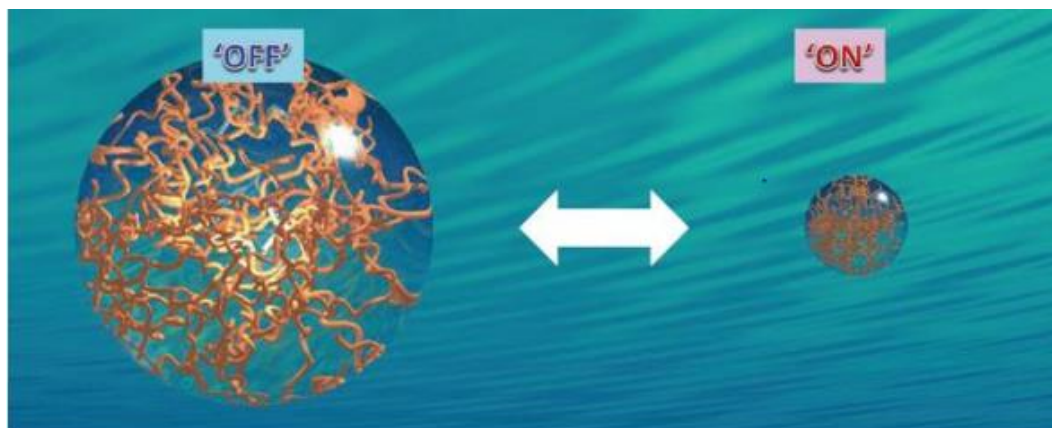


Fig. 1. 4: Schematic illustration of a hydrogel that can undergo reversible volume phase transitions upon minute changes in environmental condition

1.4.4.1 pH responsive hydrogels

Generally, pH-sensitive hydrogels that contain ionic comonomers in their polymeric backbone which is shown in fig. 1.5. The main properties of these hydrogels that make them applicable in the medical field are biocompatibility and their ability to be manipulated to be responsive to specific physiological stimuli [42]. The pH-responsive hydrogel allows significant protection of the sensitive bioactive materials, which is loaded in the polymeric matrix of the hydrogel.

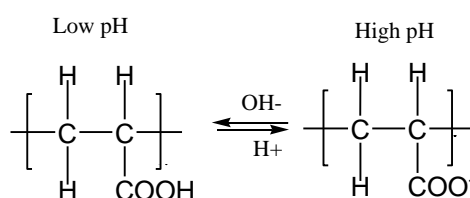


Fig. 1. 5: pH responsive hydrogel

1.4.4.2 Thermoresponsive hydrogels

Thermoresponsive hydrogels are formed above a lower critical solution temperature (LCST) where the polymer solutions undergo phase separation to form hydrogels [43-47]. At temperature below LCST, all the components in the system are completely miscible in all proportions [48]. Polymers with upper critical solution temperature (UCST) get soluble upon heating [49]. The thermoresponsive hydrogels are found to have various hydrophobic groups, and LCST/UCST can be modified by changing the ratio of hydrophilic and hydrophobic groups of the polymers [50-51]. Thermoresponsive hydrogels are of great interest in the area of biomedical applications

especially for drug delivery applications as many hydrogels show gel formation at universally accepted physiological temperature of 37°C, and also, several easy modifications are available to control gel formation at physiological temperature.

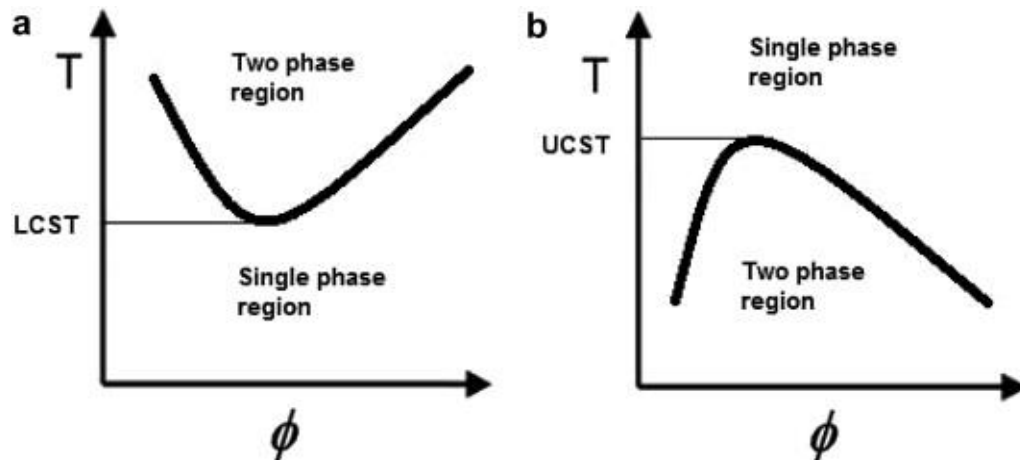


Fig. 1. 6: Positive and negative temperature responsive hydrogels

1.5 Properties of hydrogel

Hydrophilic gels called hydrogels receive considerable attention for their use in the field of pharmaceutical and biomedical engineering. This material can be used as a carrier for drug and other therapeutic bio-molecule only if it is biodegradable, biocompatible and non-toxic [52]. Thus, once the biomaterials are prepared one must evaluate the characteristic properties like swelling behavior, mechanical properties and toxicity studies, etc. so that the hydrogel could be used successfully in the concerned biomedical field.

1.5.1 Mechanical property

Mechanical properties of hydrogels are very important from the pharmaceutical and biomedical point of view. The evaluation of the mechanical property is essential in various biomedical applications viz. ligament and tendon repair, wound dressing material, the matrix for drug delivery, tissue engineering and cartilage replacement material [53-55]. The mechanical properties of hydrogels should be such that it can maintain its physical texture during the delivery of therapeutic moieties for the predetermined period of time. Changing the degree of cross-linking, the desired mechanical property of the hydrogel could be achieved.

1.5.1.1 Tensile strength

The maximum stress that a material (hydrogel) can withstand while being stretched or pulled before failing or breaking is known as tensile strength [56]. Elongation at break, also known as fracture strain, is the ratio between changed length and initial length after breakage of the test specimen [57].

On the other hand, stress is defined as a force per unit area. It has the same units as pressure, and in fact, the pressure is one special variety of stress [58]. However, stress is a much more complex quantity than pressure because it varies both with direction and with the surface, it acts on.

The strain is defined as the amount of deformation an object experiences compared to its original size and shape. For example, if a piece of hydrogel 11 cm on a side is deformed so that it becomes 10 cm long, the strain is $(11-10)/11$ or 0.1.

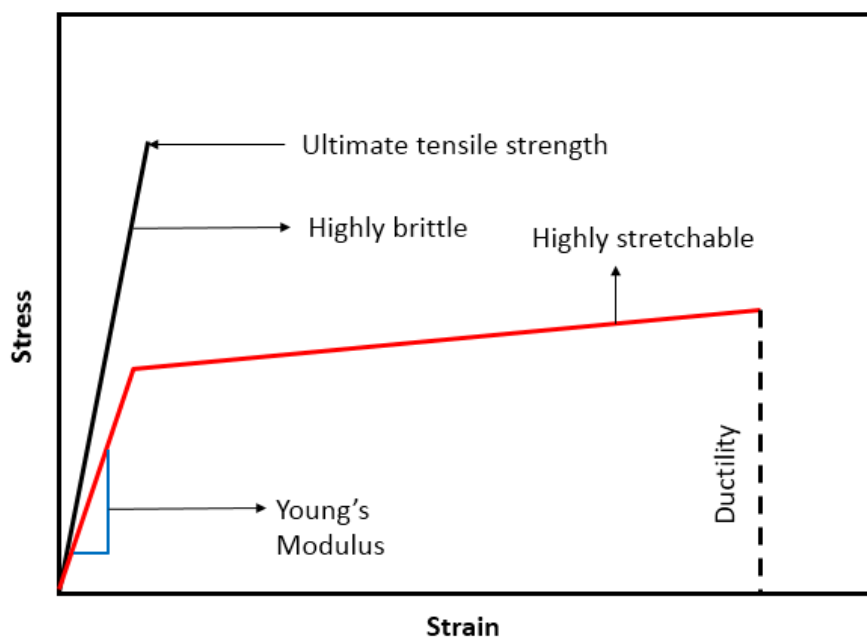


Fig. 1. 7: Stress- strain curve

The tensile strength of a material quantifies how much stress the material will endure before failing. This is very important in applications that rely upon polymer's physical strength or durability. For example, a rubber band with higher tensile strength will hold a greater weight before snapping. Usually tensile strength increases with polymer chain length in the polymer matrix [59].

1.5.1.2 Young's Modulus

Young's modulus is a mechanical property that measures the stiffness of a hydrogel. It defines the relationship between stress (force per unit area) and strain (proportional deformation) in a material in the linear elasticity regime of a uniaxial deformation [60].

It can be expressed as in the following

$$E = \sigma / \epsilon$$

Where,

- E is Young's modulus, in pascal
- σ is the uniaxial stress, or uniaxial force per unit surface, in pascal
- ϵ is the strain, or proportional deformation (change in length divided by original length) (dimensional). In practice, Young's moduli are given in megapascals (MPa or N/mm^2) or gigapascals (GPa or kN/mm^2)

1.5.1.3 Ductility

Ductility is a measure of a material's ability to undergo significant plastic deformation before rupture, which may be expressed as percent elongation or percent area reduction from a tensile test [61].

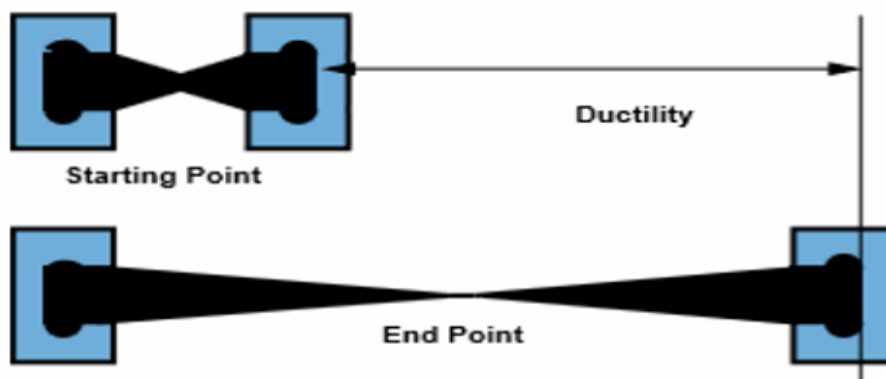


Fig. 1. 8 : Ductility test of a material

1.5.1.3 Toughness

Toughness is the property of a material that enables it to absorb and distribute within itself relatively large amounts of energy (both stresses and strains) of repeated impacts

and/or shocks, and undergo considerable deformation before fracturing or failing [62]. In one word it is the opposite of brittleness.

1.5.1.4 Mechanically strong hydrogel

In the last few decades, some types of hydrogels are established with good mechanical properties, namely topological hydrogels (TP gels), nanocomposite hydrogels (NC gels), double-network hydrogels (DN gels), and macromolecular microsphere hydrogels which have been successfully prepared via different strategies [63-64]. These strong mechanical properties hydrogels are discussed in the following segments.

1.5.1.4.1 Topological hydrogel

Topological gels are made from cross-linked polyrotaxane. Cross-linking junctions consisting of cyclic molecules can move freely in polymer networks unlike usual chemical gels and rubbers [65]. In other words, polymer chains can pass through cross-linking junctions freely to activate pulley effect into the networks. Topological gel exhibits extreme softness and strong shape recovery.

1.5.1.4.2 Double-network hydrogels (DN gels)

DN gels consisting of two networks with strongly asymmetric network structures and properties, are one of the most investigated high strength hydrogels. In most cases, the first network of DN gels is rigid, brittle and tightly crosslinked, while the second network is soft, ductile and loosely crosslinked [66-67].

1.5.1.4.3 Macromolecular microsphere (MMC) hydrogels

MMC hydrogel is a kind of tough hydrogel fabricated by using per oxidized macromolecular microspheres as polyfunctional initiating and cross-linking centers (PFICC) [68].

1.5.1.4.4 Nanocomposite hydrogel (NC gels)

NC gel consists of organic polymer and inorganic particles which improves mechanical, electrical, biological, and swelling/de-swelling properties. NC gels are of most importance because of their outstanding mechanical properties and facile synthesis [69]. They exhibit a number of new functions such as sliding frictional behaviors, abnormal hydrophobic surfaces, optical anisotropy, as well as self-healing ability. Most of these properties are attributed to their unique organic (polymer)–inorganic (clay) network structure resulted from employing the clay platelets to act as multifunctional cross-linking agents [70-72]. Inspired by the clay-based NC gels, various nanomaterials such as silica, cellulose nanocrystals and polystyrene nanoparticles are also employed to prepare nanocomposite hydrogels with novel properties. Here we choose silica as a inorganic particles because of its

- i) Large surface area
- ii) Strong surface binding energy
- iii) Due to hydrophilic silanol group, it can form hydrogen bond and electrostatic interaction with others compound.
- iv) Versatile functionalization

Here, we prepared silica-grafted nanocomposite gels by using functional silica nanoparticles as macro-crosslinkers with the AAm monomer. Herein, silica nanoparticles are modified with vinyl groups on the surface, which were copolymerized with AAm monomers, yielding PAAm-MSiO₂ hydrogel.

1.5.2 Biocompatible properties

It is important for the hydrogels to be biocompatible and nontoxic in order to make it applicable in the biomedical field. Most polymers used for this purpose must pass cytotoxicity and *in-vivo* toxicity tests [73]. Biocompatibility is the ability of a material to perform with an appropriate host response in a specific application. Biocompatibility consists basically of two elements: (a) bio-safety i.e. appropriate host response not only systemic but also local (the surrounding tissue), the absence of cytotoxicity, mutagenesis, and/or carcinogenesis and (b) bifunctionality i.e. the ability of material to

perform the specific task for which it is intended.

1.5.3 Swelling Properties

The swelling behavior of hydrogel systems is an important parameter governing their applications specifically in pharmaceutical, ophthalmology and tissue engineering [74]. The polymer chains in a hydrogel interact with the solvent molecule and tend to expand to the fully solvated state, while the crosslinked structure applies a retractive force to pull the chains inside. Equilibrium is achieved when these expanding and retracting forces counterbalance each other. The equilibrium swelling ratio or water content, given by Eq 1.1 is generally used to describe the swelling behavior of hydrogels

$$\text{Equilibrium swelling ratio} = W_{\text{swollen}}/W_{\text{dry}} \dots\dots\dots 1.1$$

Here, W_{swollen} is the weight of the swollen gel, and W_{dry} is the weight of the dry gel. The swelling kinetics of hydrogels can also be determined from the swelling curves. First, the weight of the dry gel (W_0) is determined. The dried gel was then immersed in an excess amount of water until the swelling equilibrium is attained. The weight of the wet gel (W_t) is determined after the removal of the surface water. The swelling ratio is calculated with the following equation

$$\text{Swelling ratio} = (W_t - W_0) / W_0 \dots\dots\dots 1.2$$

Many groups have investigated the swelling/shrinking kinetics of PNIPAAm gels when the temperature is increased or decreased to above or below the LCST, respectively. For example, Yoshida [75] and coworkers have compared the shrinking kinetics of PNIPAAm gels with different architectures. Comb-type PNIPAAm hydrogels collapsed from a fully swollen state in less than 20 min, whereas similar gels without grafted side chains take more than one month to undergo full shrinking [76-77]. They also reported a comb-type grafted hydrogel composed of PEO graft chains in the crosslinked PNIPAAm network [78]. The swelling characteristics are crucial to the use of hydrogels in biomedical and pharmaceutical applications since the equilibrium swelling ratio affects the solute diffusion coefficient, surface wettability, and mobility and optical and mechanical properties of the hydrogel. The swelling properties are determined by many factors, including the type and composition of monomers, crosslinking density and other environmental factors such as temperature, pH and ionic strength [79]

1.6 Application of Hydrogel

1.6.1 Drug delivery applications

Polymeric hydrogels are drawing attention since 1950s. Being blessed with the boon of smartness, it can be triggered externally and exhibits a spatiotemporal release mechanism. Owing to rapid and controllable diffusion rate, they have been considered as a promising vehicle for the encapsulation and controlled release in numerous physiological conditions, for instance, cancer therapy, osteoarthritis, diabetes, viral and bacterial infection [80], cardiac disease [81], etc. The main benefit proffered by hydrogel in drug delivery applications is their drug delivery in a controlled manner for a long period thus enabling the active pharmaceutical ingredient over a longer duration [82]. As hydrogels possess excellent property to imbibe water, that is even greater than 90% of their own weight. This unique hydrophilic property makes them classic from other drug delivery systems. Delivery of therapeutic agents from hydrogel occurs mainly through three mechanisms diffusion-controlled systems, swelling-controlled systems, and chemically controlled systems

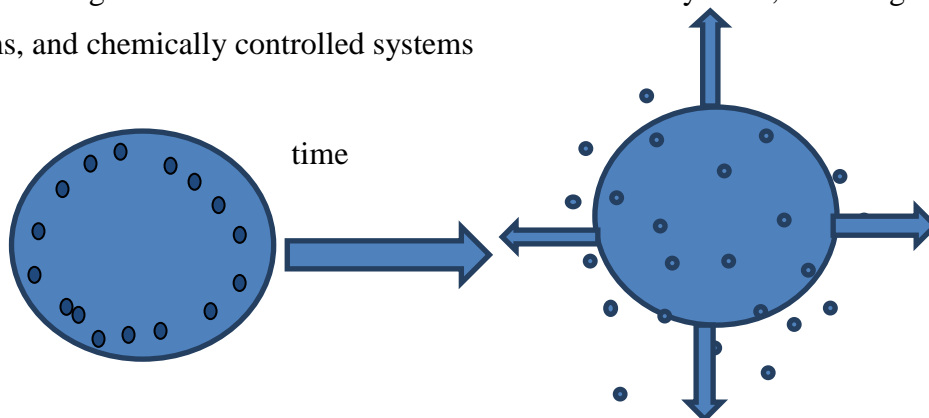


Fig. 1. 9: Drug released from hydrogel

1.6.2 Hydrogel in agriculture

Hydrogel can play an important role in agriculture because of its holding capacity of water about 400 times to their own weight and release 95% of that to growing plants for the properties of crosslinking in hydrogel [83]. By using the hydrogel in the soil which improves physical properties of soil to:

- i) Increase water holding capacity
- ii) Increase water use efficiency
- iii) Drought stress reduction
- iv) Enhance soil permeability and infiltration rate

- v) Reduce irrigation frequency
- vi) Enhanced fertilizer efficiency
- vii) Reduce compaction tendency Stop soil erosion, farm run-off & surface leaching
- Viii) Increase plant performance, particularly in structure-less soils stressed with drought condition

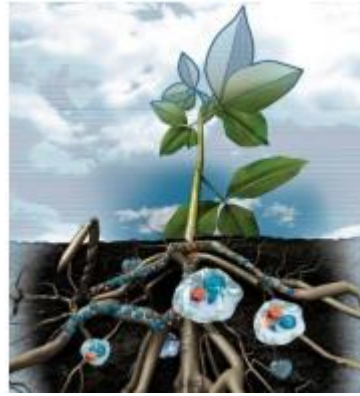


Fig. 1. 10 : Hydrogel in agriculture

1.7 Literature Review

Hydrogels have received considerable attention in the last few decades owing to their applications in different fields. They have widely been used in the fields such as drug delivery system [84], sensors [85], actuators, biomaterials and so on. But the potential applications of the hydrogel are often limited by their poor mechanical performances, for example too weak or brittle in nature, low toughness, low stretching and bending ability, low elastic modulus, etc. In order to overcome these limitations, different strategies including sliding hydrogels, nanocomposite hydrogels, double network hydrogels have been reported which are they formed through covalent bonds, hydrogen bonds, Van der Waals interactions and physical entanglements [86]. Among them, inorganic nanocomposite hydrogels have gained much attention owing to the remarkable properties that can be obtained by a combination of the organic and inorganic components into the network. Recently, Haraguchi et al [87] prepared nanocomposite hydrogel (NC gels) by using clay nanoparticles as a crosslinker which exhibits high mechanical strength, rapid temperature-response and a high degree of swelling. The optical, mechanical and swelling/de-swelling properties of NC gels can be controlled by changing the gel composition and clay nanoparticles. So far, nanocomposite hydrogels have been prepared *via* grafting of polymers onto the surface of inorganic components using weak ionic forces to show attractive mechanical, thermal, optical, electrical and magnetic properties for their diverse application in

plastics and rubber reinforcement, coatings, catalyst, and diagnostics tools. But these hydrogel network disrupt at suitable solvent and at harsh condition. Here, the strategy for designing silica nanocomposite hydrogels will be followed *via* strong covalent interactions between inorganic and organic components in which the crosslinking density and inter-crosslinking distance can be controlled independently to improve their mechanical properties. Silica-based nanocomposite has extraordinary characteristics [88]. Therefore, modified narrow dispersed silica cross-linker as described in the proposal are expected to overcome the drawbacks of the traditionally cross-linked via weak ionic interactions NC hydrogels.

1.8 Research Goal

The core aim of the research is to fabricate modified narrow dispersed silica -cross-linked polymeric hydrogels for improved mechanical properties. Vinyl functionalized silica will be synthesized and consequently used as a 2D cross-linker in the in-situ polymerization of acrylamide. The aims of this research are:

- i) To synthesize modified silica nanoparticles as crosslinker
- ii) To fabricate mechanically strong hydrogel using synthesized cross-linker which can covalently bind with long polymer chains
- iii) To investigate the mechanical properties of synthesized hydrogels with varying cross-linker amount, the concentration of AAm and silica particle sizes.
- iv) To eliminate the drawbacks of physically bonded conventional NC hydrogels

1.9 References

- [1] L. Ye, Y. Tang, and D. Qiu, 'Enhance the mechanical performance of polyacrylamide hydrogel by aluminium-modified colloidal silicanhan,' *Colloids Surfaces A Physicochem. Eng. Asp.*, vol. 447, pp. 10," *Colloids Surfaces A Physicochem. Eng. Asp.*, vol. 447, pp. 103–110, (2014).
- [2] J. Maitra and V. K. Shukla, "Cross-linking in Hydrogel - A Review," *Am. J. Polym. Sci.*, vol. 25, pp 2163-1342 (2014).
- [3] Wichterle, O. and Lim, D. "Hydrophilic Gels for Biological Use,". *Nature*, vol.185, pp. 117-118, 1960.
- [4] M. B. Mellott, K. Searcy, and M. V. Pishko, "Release of protein from highly cross-linked hydrogels of poly(ethylene glycol) diacrylate fabricated by UV polymerization," *Biomaterials*, vol. 22, pp. 929-941 (2001).
- [5] X. Zhang, G. Lin, S. R. Kumar, and J. E. Mark, "Hydrogels prepared from polysiloxane chains by end linking them with trifunctional silanes containing hydrophilic groups," *Polymer (Guildf)*., vol. 50, pp. 5414–5421 (2009).
- [6] R. Guo, Q. Su, J. Zhang, A. Dong, C. Lin, and J. Zhang, "Facile Access to Multisensitive and Self-Healing Hydrogels with Reversible and Dynamic Boronic Ester and Disulfide Linkages," *Biomacromolecules*, vol. 18, pp. 1356–1364 (2017).
- [7] F. Rossi, G. Perale, G. Storti, and M. Masi, "A library of tunable agarose carbomer-based hydrogels for tissue engineering applications: The role of cross-linkers," *J. Appl. Polym. Sci.*, vol.123, pp. 2211-2221 (2012).
- [8] S. Deshmukh, D. A. Mooney, and J. M. D. MacElroy, "Molecular simulation study of the effect of cross-linker on the properties of poly(N-isopropyl acrylamide) hydrogel," *Mol. Simul.*, vol. 37, pp.846-854 (2011).
- [9] S. Liu *et al.*, "Polysaccharide-templated preparation of mechanically-tough, conductive and self-healing hydrogels," *Chem. Eng. J.*, vol.334, pp. 2220-2230 (2018).
- [10] Bilotti, E. and Mary, Q., "*Polymer/Sepiolite Clay Nanocomposites*," PhD . thesis, School of Engineering and Materials Science, University of London, 2009.

- [11] S. Van Vlierberghe, P. Dubruel, and E. Schacht, "Biopolymer-based hydrogels as scaffolds for tissue engineering applications: A review," *Biomacromolecules*, vol. 12, pp.1287-1408 (2011).
- [12] E. Caló and V. V. Khutoryanskiy, "Biomedical applications of hydrogels: A review of patents and commercial products," *European Polymer Journal*, vol. 65, pp. 252-267 (2015).
- [13] K. Shaini, "Preparation method, Properties and Crosslinking of hydrogel: a review," *PharmaTutor*, vol. 5, pp. 27-36(2017).
- [14] M. F. Akhtar, M. Hanif, and N. M. Ranjha, "Methods of synthesis of hydrogels A review," *Saudi Pharmaceutical Journal*. Vol. 24, pp. 554-559 (2016).
- [15] N. Bhattarai, J. Gunn, and M. Zhang, "Chitosan-based hydrogels for controlled, localized drug delivery.," *Adv. Drug Deliv. Rev.*, vol. 62 pp.83-99 (2010).
- [16] J. R. Hughey, J. M. Keen, D. A. Miller, K. Kolter, N. Langley, and J. W. McGinity, "The use of inorganic salts to improve the dissolution characteristics of tablets containing Soluplus®-based solid dispersions," *Eur. J. Pharm. Sci.*, vol. 48, pp. 758-766 (2013).
- [17] H. Tsuji, "Poly(lactide) stereocomplexes: Formation, structure, properties, degradation, and applications," *Macromolecular Bioscience*. Vol. 5, pp.559-579 (2005).
- [18] C. M. Hassan and N. A. Peppas, "Structure and Applications of Poly(vinyl alcohol) Hydrogels Produced by Conventional Crosslinking or by Freezing/Thawing Methods," *Biopolym. · PVA Hydrogels, Anionic Polym. Nanocomposites*, vol. 153, pp. 37-65 (2007).
- [19] L. Cai, R. E. Dewi, and S. C. Heilshorn, "Injectable hydrogels with in situ double network formation enhance retention of transplanted stem cells," *Adv. Funct. Mater.*, vol. 25, pp. 1344-1351 (2015).
- [20] I. C. Alupeii, M. Popa, M. Hamcerencu, and M. J. M. Abadie, "Superabsorbant hydrogels based on xanthan and poly(vinyl alcohol): The study of the swelling properties," *Eur. Polym. J.*, vol. 38, pp. 2313-2320 (2002).

- [21] W. E. Hennink and C. F. van Nostrum, "Novel crosslinking methods to design hydrogels," *Advanced Drug Delivery Reviews*, vol. 64, pp. 223-236 (2012).
- [22] V. D. Athawale and V. Lele, "Graft copolymerization onto starch. II. Grafting of acrylic acid and preparation of its hydrogels," *Carbohydr. Polym.*, vol. 35, pp. 21-25 (1998).
- [23] M. C. Clochard *et al.*, "Tailoring bulk and surface grafting of poly(acrylic acid) in electron-irradiated PVDF," *Polymer (Guildf)*, vol. 35, pp. 8683-8693 (2004).
- [24] T. Jayaramudu, G. M. Raghavendra, K. Varaprasad, K. M. Raju, E. R. Sadiku, and J. Kim, "5-Fluorouracil encapsulated magnetic nanohydrogels for drug-delivery applications," *J. Appl. Polym. Sci.*, vol. 133, pp. 1-10 (2016).
- [25] T. Jayaramudu, G. M. Raghavendra, K. Varaprasad, R. Sadiku, and K. M. Raju, "Development of novel biodegradable Au nanocomposite hydrogels based on wheat: For inactivation of bacteria," *Carbohydr. Polym.*, vol. 92, pp. 2193-2200 (2013).
- [26] Z. Yang, H. Peng, W. Wang, and T. Liu, "Crystallization behavior of poly(ϵ -caprolactone)/layered double hydroxide nanocomposites," *J. Appl. Polym. Sci.*, vol. 116, pp. 2658-2667 (2010).
- [27] A. E. J. De Nooy, G. Masci, and V. Crescenzi, "Versatile Synthesis of Polysaccharide Hydrogels Using the Passerini and Ugi Multicomponent Condensations," *Macromolecules*, vol. 32, pp. 1318-1320 (1999).
- [28] A. E. J. De Nooy, D. Capitani, G. Masci, and V. Crescenzi, "Ionic polysaccharide hydrogels via the Passerini and Ugi multicomponent condensations: Synthesis, behavior and solid-state NMR characterization," *Biomacromolecules*, vol. 1, pp. 259-267 (2000).
- [29] R. Y. Tsien and A. Miyawaki, "Seeing the machinery of live cells," *Science*, vol. 280, pp. 1954-1955 (1998).
- [30] A. Das *et al.*, "Ionic Modification Turns Commercial Rubber into a Self-Healing Material," *ACS Appl. Mater. Interfaces*, vol. 7, pp. 20623-20630 (2015).
- [31] H. Chung, P. Glass, J. M. Pothen, M. Sitti, and N. R. Washburn, "Enhanced adhesion of dopamine methacrylamide elastomers via viscoelasticity tuning," *Biomacromolecules*, vol. 12, pp. 342-347 (2011).

- [32] P. Gamage, J. P. Deville, and J. Sherman, "Solids-Free Fluid-Loss Pill for High-Temperature Reservoirs," *SPE Drill. Complet.*, vol. 29, pp. 125-130 (2014).
- [33] J. T. Oliveira and R. L. Reis, "Hydrogels from polysaccharide-based materials: Fundamentals and applications in regenerative medicine," in *Natural-Based Polymers for Biomedical Applications*, vol. 2 pp. 485-514 (2008).
- [34] K. Qiu and A. N. Netravali, "Fabrication and characterization of biodegradable composites based on microfibrillated cellulose and polyvinyl alcohol," *Compos. Sci. Technol.*, vol. 72, pp. 1588-1594 (2012).
- [35] J. E. Eldridge and J. D. Ferry, "Studies of the cross-linking process in gelatin gels. III. Dependence of melting point on concentration and molecular weight," *J. Phys. Chem.*, vol. 54, pp. 992-996 (1954).
- [36] K. W. M. Boere *et al.*, "Covalent attachment of a three-dimensionally printed thermoplast to a gelatin hydrogel for mechanically enhanced cartilage constructs," *Acta Biomater.*, vol. 10, pp. 2602-2611 (2014).
- [37] D. A. Gyles, L. D. Castro, J. O. C. Silva, and R. M. Ribeiro-Costa, "A review of the designs and prominent biomedical advances of natural and synthetic hydrogel formulations," *European Polymer Journal*, vol. 88, pp. 373-392 (2017).
- [38] E. Sandoz-Rosado, T. D. Beaudet, J. W. Andzelm, and E. D. Wetzel, "High strength films from oriented, hydrogen-bonded 'graphamid' 2D polymer molecular ensembles," *Sci. Rep.*, vol. 8, pp. 3708-3718 (2018).
- [39] Imran, A. B., Seki, T., Takeoka, Y. "Recent Advances in Hydrogels in Terms of Fast Stimuli Sensitivity and Mechanical Strength" *Polymer Journal (Nature Publishing Group, United Kingdom)* 42, 839–851 (2010)
- [40] I. Willner, "Stimuli-Controlled Hydrogels and Their Applications," *Acc. Chem. Res.*, vol. 50, pp. 657-658 (2017)
- [41] W. Guo *et al.*, "Reversible Ag⁺-crosslinked DNA hydrogels," *Chem. Commun.*, vol. 50, pp. 4065-4068 (2014).
- [42] M. Preis and J. M. Rosenholm, "Printable nanomedicines: the future of customized drug delivery?," *Ther. Deliv.*, vol. 8, pp. 721-723 (2017).

- [43] F. Lin *et al.*, “Peptide-Functionalized Oxime Hydrogels with Tunable Mechanical Properties and Gelation Behavior,” *Biomacromolecules*, vol.14, pp. 3749-3758 (2013).
- [44] M. Hamalainen, B. Mohajeri, and T. Nyberg, “Removing barriers to sustainability research on personal fabrication and social manufacturing,” *J. Clean. Prod.*, vol. 80, pp. 666-681 (2018).
- [45] H. A. Gaballa, L. M. Geever, J. A. Killion, and C. L. Higginbotham, “Synthesis and characterization of physically crosslinked N-vinylcaprolactam, acrylic acid, methacrylic acid, and N,N-dimethylacrylamide hydrogels,” *J. Polym. Sci. Part B Polym. Phys.*, vol. 51, pp. 1555-1564 (2013).
- [46] V. I. Lozinsky *et al.*, “Synthesis of N-vinylcaprolactam polymers in water-containing media,” *Polymer (Guildf)*, vol.41 pp.6507-6518 (2000).
- [47] A. Tél, R. A. Bauer, Z. Varga, and M. Zrínyi, “Heat conduction in poly(N-isopropylacrylamide) hydrogels,” *Int. J. Therm. Sci.*, vol.85, pp.47-53 (2014).
- [48] Q. Zhang and R. Hoogenboom, “Polymers with upper critical solution temperature behavior in alcohol/water solvent mixtures,” *Progress in Polymer Science*, vol. 48, pp. 122-142 (2015).
- [49] Y. Jin, Y. Shen, J. Yin, J. Qian, and Y. Huang, “Nanoclay-Based Self-Supporting Responsive Nanocomposite Hydrogels for Printing Applications,” *ACS Appl. Mater. Interfaces*, vol.10, pp. 10461-10470 (2018).
- [50] F. Hapiot, S. Menuel, and E. Monflier, “Thermoresponsive hydrogels in catalysis,” *ACS Catalysis*, vol.3, pp.1006-1010 (2013).
- [51] A. Haider, S. Haider, S. S. Han, and I. K. Kang, “Recent advances in the synthesis, functionalization and biomedical applications of hydroxyapatite: a review,” *RSC Advances*, vol.7, pp.7442-7458 (2017).
- [52] T. Garg, O. Singh, S. Arora, and R. Murthy, “Scaffold: a novel carrier for cell and drug delivery,” *Crit. Rev. Ther. Drug Carrier Syst.*, vol. 29 pp.1-63 (2012).
- [53] C. Chaudhary and T. Garg, “Scaffolds: A Novel Carrier and Potential Wound Healer,” *Crit. Rev. Ther. Drug Carrier Syst.*, vol.32, pp.277-321 (2015).
- [54] N. C. Hunt and L. M. Grover, “Cell encapsulation using biopolymer gels for regenerative medicine,” *Biotechnology Letters*, vol. 32, pp.733-742 (2010).

- [55] S. I. Durowaye, G. I. Lawal, M. A. Akande, and V. O. Durowaye, “Mechanical Properties of Particulate Coconut Shell and Palm Fruit Polyester Composites,” *Int. J. Mater. Eng.*, vol.4, pp.141-147 (2014).
- [56] J. T. Wang *et al.*, “Effects of laser shock peening on stress corrosion behavior of 7075 aluminum alloy laser welded joints,” *Mater. Sci. Eng. A*, vol.647, pp.7-14 (2015).
- [57] V. De Vita and G. Fabbrocini, “Mechanical Stress as a Cause of Hidradenitis Suppurativa: A Lesson from a Patient with a Monster Hernia.,” *Acta Dermatovenerol. Croat.*, vol. 26, pp.260-261 (2018).
- [58] T. Wang, A. B. Dalton, and J. L. Keddie, “Importance of molecular friction in a soft polymer-nanotube nanocomposite,” *Macromolecules*, vol.51 pp.7656-7661 (2008).
- [59] E. Aasprong, O. Smidsrød, and B. T. Stokke, “Swelling, mechanical properties and effect of annealing of scleroglucan gels,” *Carbohydr. Polym.*, vol.60, pp. 363-378 (2005).
- [60] C. C. Koch, D. G. Morris, K. Lu, and A. Inoue, “Ductility of nanostructured materials,” *MRS Bull.*, vol. 24, pp. 54-58 (1999).
- [61] X. Luo, J. yu Xu, E. lei Bai, and W. Li, “Mechanical properties of ceramics-cement based porous material under impact loading,” *Mater. Des.*, vol.55 pp.778-784 (2014).
- [62] F. Li *et al.*, “Strong Wet Adhesion of Tough Transparent Nanocomposite Hydrogels for Fast Tunable Focus Lenses,” *ACS Appl. Mater. Interfaces*, vol. 11, pp.15071-15078 (2019).
- [63] S. Naficy, H. R. Brown, J. M. Razal, G. M. Spinks, and P. G. Whitten, “Progress Toward Robust Polymer Hydrogels,” *Aust. J. Chem.*, vol.64, pp.1007-1025 (2011).
- [64] T. Huang, H. Xu, K. Jiao, L. Zhu, H. R. Brown, and H. Wang, “A novel hydrogel with high mechanical strength: A macromolecular microsphere composite hydrogel,” *Adv. Mater.*, vol. 29, pp. 1622-1626 (2007).
- [65] J. Yang, Y. Li, L. Zhu, G. Qin, and Q. Chen, “Double network hydrogels with controlled shape deformation: A mini review,” *J. Polym. Sci. Part B Polym. Phys.*, vol. 56, no. 19, pp. 1351–1362 (2018).

- [66] Q. Chen *et al.*, “Improvement of Mechanical Strength and Fatigue Resistance of Double Network Hydrogels by Ionic Coordination Interactions,” *Chem. Mater.*, vol. 28, pp.5710-5720 (2016).
- [67] F. Jiang, T. Huang, C. He, H. R. Brown, and H. Wang, “Interactions affecting the mechanical properties of macromolecular microsphere composite hydrogels,” *J. Phys. Chem. B*, vol. 117, no. 43, pp. 13679–13687 (2013).
- [68] C. Pan, L. Liu, Q. Chen, Q. Zhang, and G. Guo, “Tough, Stretchable, Compressive Novel Polymer/Graphene Oxide Nanocomposite Hydrogels with Excellent Self-Healing Performance,” *ACS Appl. Mater. Interfaces*, vol. 9, pp.38052-38061 (2017).
- [69] K. Haraguchi, H. J. Li, K. Matsuda, T. Takehisa, and E. Elliott, “Mechanism of forming organic/inorganic network structures during in-situ free-radical polymerization in PNIPA-clay nanocomposite hydrogels,” *Macromolecules*, vol. 38, pp.3482-3490 (2005).
- [70] J. E. Lee, N. Lee, T. Kim, J. Kim, and T. Hyeon, “Multifunctional mesoporous silica nanocomposite nanoparticles for theranostic applications,” *Acc. Chem. Res.*, vol.44, pp. 893-902 (2011).
- [71] L. Xue, J. Li, J. Fu, and Y. Han, “Super-hydrophobicity of silica nanoparticles modified with vinyl groups,” *Colloids Surfaces A Physicochem. Eng. Asp.*, vol.338, pp.15-19 (2009).
- [72] B. Ekwall *et al.*, “MEIC evaluation of acute systemic toxicity - Part VI. The prediction of human toxicity by rodent LD50 values and results from 61 in vitro methods,” *Atla-Alternatives to Lab. Anim.*, vol.26, pp. 617-658 (1998).
- [73] J. Radwan-Pragłowska *et al.*, “Microwave-assisted synthesis and characterization of bioactive chitosan scaffolds doped with Au nanoparticles for mesenchymal stem cells culture,” *Int. J. Polym. Mater. Polym. Biomater.*, vol.68 pp. 351-359 (2019).
- [74] H. Zhang, X. Guo, J. Wu, D. Fang, and Y. Zhang, “Soft mechanical metamaterials with unusual swelling behavior and tunable stress-strain curves,” *Sci. Adv.*, vol.4, pp. 1-10 (2018).

- [75] H. Tajima, Y. Yoshida, and K. Yamagiwa, "Experimental study of swelling and shrinking kinetics of spherical poly(N,N-diethylacrylamide) gel with continuous phase transition," *Polymer (Guildf)*, vol. 52, pp. 732-738 (2011).
- [76] H. K. Ju, S. Y. Kim, and Y. M. Lee, "pH/temperature-responsive behaviors of semi-IPN and comb-type graft hydrogels composed of alginate and poly(N-isopropylacrylamide)," *Polymer (Guildf)*, vol. 42, pp. 6851-6857 (2001).
- [77] H. Tan, C. M. Ramirez, N. Miljkovic, H. Li, J. P. Rubin, and K. G. Marra, "Thermosensitive injectable hyaluronic acid hydrogel for adipose tissue engineering," *Biomaterials*, vol.30, pp. 6844-6853 (2009).
- [78] Y. Kaneko *et al.*, "Deswelling mechanism for comb-type grafted poly(N-isopropylacrylamide) hydrogels with rapid temperature responses," *Polym. Gels Networks*, vol.6, pp. 333-345 (1998).
- [79] S. J. Tan, J. Y. Fang, Z. Yang, M. E. Nimni, and B. Han, "The synergetic effect of hydrogel stiffness and growth factor on osteogenic differentiation," *Biomaterials*, vol. 35, pp.5294-5306 (2014).
- [80] W. Gao *et al.*, "Hydrogel containing nanoparticle-stabilized liposomes for topical antimicrobial delivery," *ACS Nano*, vol.25 pp.2900-2907 (2014).
- [81] R. M. Wang and K. L. Christman, "Decellularized myocardial matrix hydrogels: In basic research and preclinical studies," *Advanced Drug Delivery Reviews*. Vol.15 pp.77-82 (2016).
- [82] M. Hamidi, K. Rostamizadeh, and M. A. Shahbazi, "Hydrogel Nanoparticles in Drug Delivery," in *Intelligent Nanomaterials: Processes, Properties, and Applications*, vol.5 pp.583-624 (2012).
- [83] M. R. Guilherme *et al.*, "Superabsorbent hydrogels based on polysaccharides for application in agriculture as soil conditioner and nutrient carrier: A review," *European Polymer Journal*.vol.72, pp. 365-385 (2015).
- [84] T. R. Hoare and D. S. Kohane, "Hydrogels in drug delivery: Progress and challenges," *Polymer*. vol.59, pp. 1993-2007 (2008).

- [85] D. Zhai *et al.*, “Highly sensitive glucose sensor based on Pt nanoparticle/polyaniline hydrogel heterostructures,” *ACS Nano*, vol. 7, pp.3540-3546 (2013).
- [86] C. Maity, W. E. Hendriksen, J. H. Van Esch, and R. Eelkema, “Spatial structuring of a supramolecular hydrogel by using a visible-light triggered catalyst,” *Angew. Chemie - Int. Ed.*, vol. 54, pp. 998-1001 (2015).
- [87] K. Haraguchi, "Nanocomposite Gels: New Advanced Functional Soft Materials". *Macromolecular Symposia.*, vol. 256, pp. 120–130 (2007)
- [88] P. Manoharan and K. Naskar, “Exploring a highly dispersible silica-elastomer composite for tire applications,” *J. Appl. Polym. Sci.*, vol.133, pp.1-10 (2016).

Chapter 2

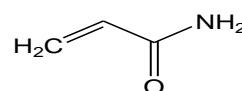
Experimental

2.1. Materials and instruments

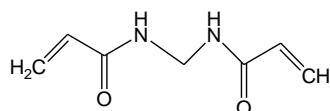
2.1.1. Chemicals

All chemicals and reagents used in this research were analytical grade and used without further purification. Deionized water was used as solvent to prepare most of the solutions of this work. The main chemicals which were used in this research are given below:

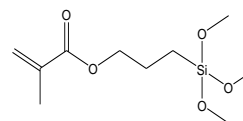
➤ Acrylamide (AAM)



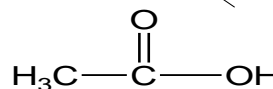
➤ *N,N*-methylenebisacrylamide (BIS)



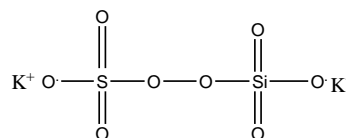
➤ 3-Methacryloxypropyltrimethoxysilane (MPTS)



➤ Acetic acid (CH₃COOH)



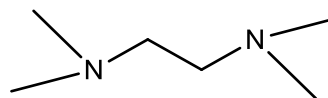
➤ Potassium persulfate (KPS)



➤ Ethanol (CH₃CH₂OH)

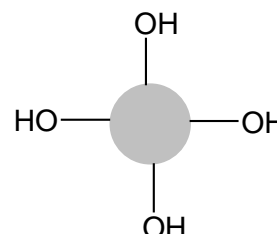


➤ Tetramethylethylenediamine (TEMED)



➤ Deionized water

➤ Silica



2.1.2. Instrument

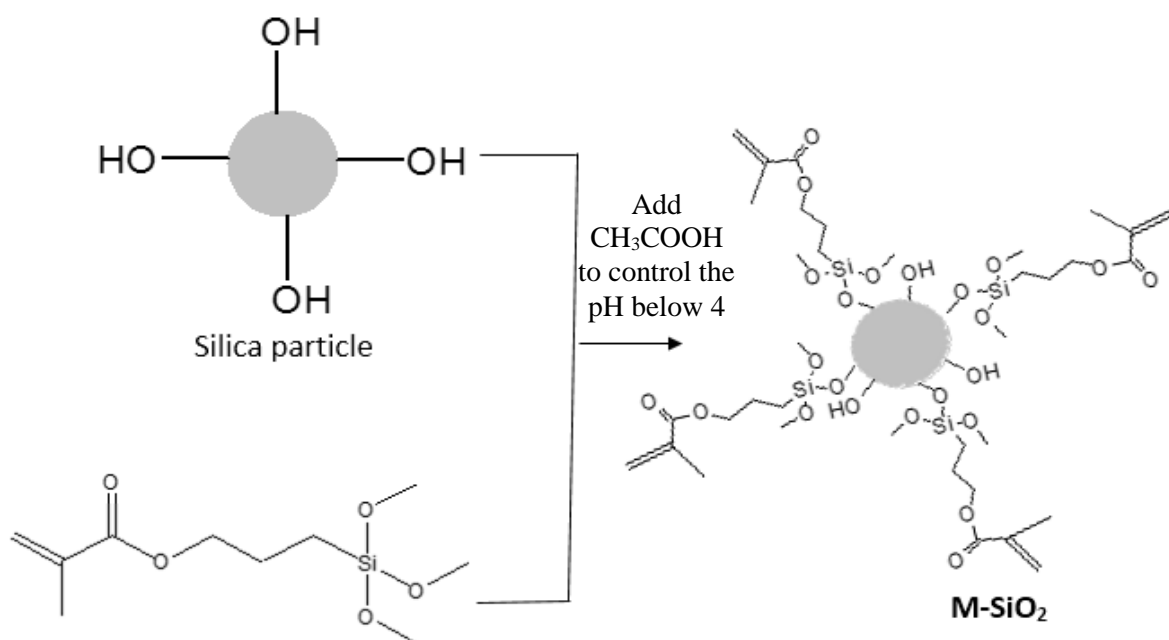
The characterizations of the samples were performed using the following instruments:

- Field emission-scanning electron microscopy (JSM-7600F, Tokyo, Japan)
- Fourier transform infrared spectrophotometer (FTIR-8400, SHIMADZU, Japan)
- Nuclear Magnetic Resonance (BPX -400, Bruker, Germany)
- Universal testing machine (100P250-12, Test resources, USA)
- Centrifuge machine (Hettich, Universal 16A)
- pH meter (Hanna, HI 8424, Romania)
- Digital balance (AB 265/S/SACT, METTLER, Toledo, Switzerland)
- Freeze dryer (Heto FD3, Denmark)
- Oven (Lab Tech, LDO-030E, Korea)
- Immersion bath circulator (LCB-R08, Korea)

2.2. Method of preparation

2.2.1. Preparation of modified silica particles (MSiO_2)

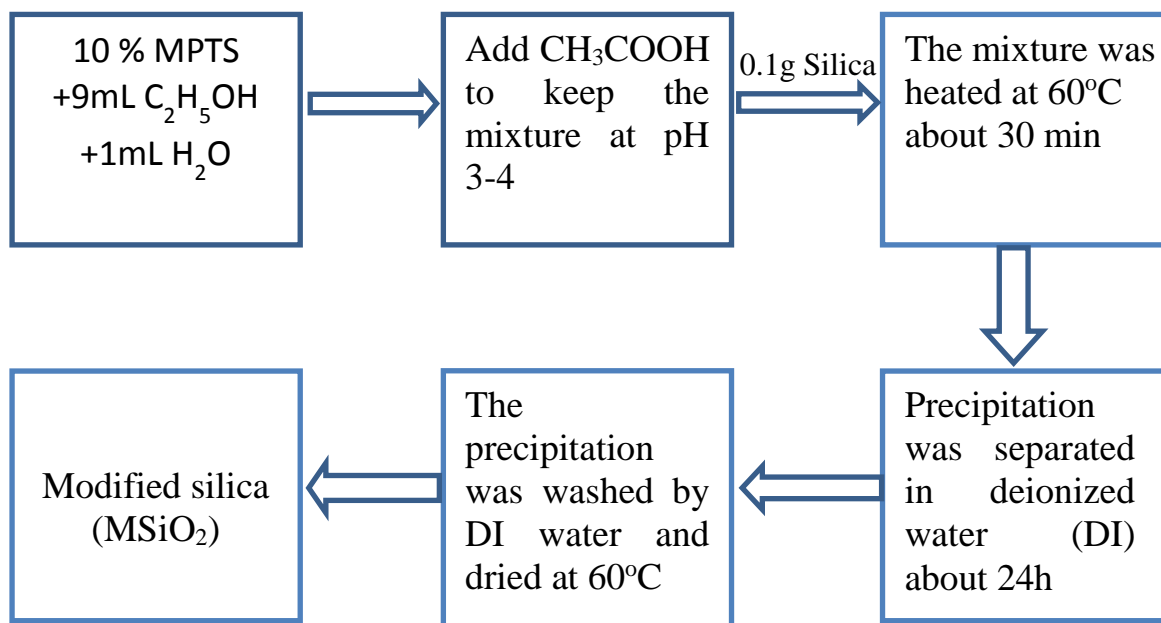
The silica particles having different sizes (100nm, 200nm and 300nm) were modified by 3-methacryloxypropyltrimethoxysilane (MPTS). MPTS (10% w/w silica) was added into ethanol–water solution (9:1 vol.%) to hydrolyze it sufficiently [1-2]. The pH of the solution was adjusted to 3–4 by using acetic acid solution (0.1 molL^{-1}). The hydrophilic silica particles were added into the solution. The mixture was then heated at 60–70°C in an oil bath and stirred at 500 rpm for 30 min. Afterwards, the particles were centrifuged and separated, and the salinized product was immersed in deionized water for 24 h. The product was washed several times with deionized water to eliminate the influence of physical adsorption. Finally, the salinized silica particles were dried at 60°C for 24 h until reach to a constant weight to obtain MSiO_2 .



3 -Methacryloxypropyltrimethoxysilane(MPTS)

Fig 2. 1: Preparation strategy of MSiO₂ as cross linker

2.2.2.(i) Schematic diagram for preparation of MSiO₂



2.2.2.(ii) General preparation scheme of MSiO₂Fig. 2. 1: Synthesis route of modified silica (MSiO₂)2.2.3. Preparation of MSiO₂ nanocomposite hydrogels

Nanocomposite hydrogel was prepared by the free radical crosslinking polymerization of AAm in presence of MSiO₂ suspension [3-4]. First, the different weight percentage of MSiO₂ with respect to AAm was prepared in distilled water. The fixed molar concentration of AAm was added to MSiO₂ solution, Table 2.1, 2.2, 2.3 and 2.4 describes the different formulation/recipe used in this work. Under nitrogen gas atmosphere, the solution was poured into a mold fabricated by spacing two glass plates with a 2 mm teflon spacer and into the glass tube. The mold and the glass tube were kept in an ice water bath and complete polymerization was carried out for 24 h at room temperature. Finally, we got AAm-MSiO₂ (200 nm silica) nanocomposite hydrogel. Different concentration of AAm (3M, 4M and 5M) and fixed amount of MSiO₂ where silica particles were 100nm, 200nm, and 300nm also used for the preparation of others AAm-MSiO₂ nanocomposite hydrogels. The crosslinking of AAm hydrogels was also carried out by using different concentration of traditional crosslinker MBA. The recipe

to fabricate different types of AAm- MSiO₂, AAm-BIS, and AAm-BIS-MSiO₂ with varying the different concentration of monomers while other gel precursors (e.g. cross-linker, initiator and solvent) remain fixed are given below.

2.2.4. Preparation recipe of different hydrogels

Table 2. 1: Preparation recipe of AAm-BIS hydrogels

Sample code	Acrylamide (M)	BIS (mM)	KPS (mM)	TEMED (μ L)
A ₂ B ₂₀	2.00	20	2.96	20
A ₂ B ₂₅	2.00	25	2.96	20
A ₂ B ₅₀	2.00	40	2.96	20
A ₂ B ₁₀₀	2.00	100	2.96	20
A ₄ B ₂₀	4.00	20	2.96	20

Where A₂ represents the acrylamide with concentration 2 and B₂₀, B₂₅, B₅₀, and B₁₀₀ illustrate the varying concentration of *N,N*-methylenebisacrylamide (BIS).

Table 2. 2: Preparation recipe of AAm-BIS- MSiO₂ hydrogels

Sample code	Acrylamide (M)	BIS (mM)	MSiO ₂ (%)	KPS (mM)	TEMED (μ L)
A ₂ S _{0.50%} B _{.7}	2.00	20	0.50	2.96	20
A ₂ S _{0.75%} B _{.7}	2.00	25	0.75	2.96	20
A ₂ S _{1.00%} B _{.7}	2.00	40	1.00	2.96	20
A ₂ S _{1.25%} B _{.7}	2.00	100	1.25	2.96	20
A ₂ S _{1.50%} B _{.7}	4.00	40	1.50	2.96	20

Where A_2 represents the acrylamide with concentration 2 and $S_{0.5\%}$, $S_{0.75\%}$, $S_{1.00\%}$, $S_{1.25\%}$ and $S_{1.50\%}$ illustrate weight % of the modified silica with respect to acrylamide. $B_{0.7}$ denotes the *N,N*-methylenebisacrylamide (BIS) with concentration of 0.7mM

Table 2. 3: Preparation recipe of AAm-MSiO₂ hydrogel

Sample code	Acrylamide (M)	MSiO ₂ (%)	KPS (mM)	TEMED (μL)
A ₄ S _{0.50%}	4.00	0.50	2.96	20
A ₄ S _{0.75%}	4.00	0.75	2.96	20
A ₄ S _{1.00%}	4.00	1.00	2.96	20
A ₄ S _{1.25%}	4.00	1.25	2.96	20

Where A_4 , represents the acrylamide with concentration 4 and $S_{0.5\%}$, $S_{0.75\%}$, $S_{1.00\%}$ and $S_{1.25\%}$ illustrate weight % of the modified silica with respect to acrylamide

Table 2. 4 : Preparation recipe of AAm-MSiO₂ hydrogel for different silica size particles: 100nm, 200nm and 300nm

Sample no.	Acrylamide (M)	MSiO ₂ (%)	KPS (mM)	TEMED (μL)
A ₃ S _{117.5}	3.00	0.75	2.96	20
A ₄ S _{216.5}	4.00	0.75	2.96	20
A ₅ S _{311.5}	5.00	0.75	2.96	20

Where A_3 , A_4 , A_5 represents the acrylamide with varying concentration 3,4 and 5. $S_{117.5}$, $S_{216.5}$, and $S_{311.5}$ illustrate the modified silica with varying particle size 117.5nm, 216.5nm and 311.5nm.

2.3 Characterizations

2.3.1. Fourier transform infrared (FTIR) spectroscopy analysis

FT-IR spectroscopy was employed to investigate the functional groups of the particles. Here, silica (SiO_2) and MSiO_2 were investigated in FTIR spectrophotometer in the region of $4000\text{--}1000\text{ cm}^{-1}$. The samples were oven-dried at 60°C and a small portion of samples were taken into vials. FTIR spectra of the solid and powdered samples were observed by mixing and grinding of samples with dry and pure KBr crystals. The mixing and grinding were done in a mortar by a pestle. The powder mixture was then compressed by manual press machine under a pressure of 8–10 tons to make a pellet. The pellet was then placed in sample chamber for measurements.

2.3.2. Nuclear magnetic resonance (NMR) analysis

^1H -NMR spectra were recorded by Bruker BPX -400 spectrometer (400 MHz) and CDCl_3 used as a solvent, tetramethylsilane (TMS) used an internal standard. All chemical shifts (δ) were recorded in ppm and coupling constant (j) in Hz. Chemical shifts were recorded relative to tetramethylsilane (TMS) peak and solvent peaks is at 7.28 ppm. Abbreviations used in the ^1H -NMR spectra are as follows s for singlet, d for doublet, t for triplet and q for quartet.

2.3.3. Field emission scanning electron microscopy (FE-SEM)

The surface morphology of the different sizes SiO_2 particles and MSiO_2 particles were conducted using FE-SEM. For, FE-SEM analysis the sample was taken into a vial and dried at the oven. Platinum was sputtered on the sample to ensure the conductivity of the sample surface. The sample is then mounted to a sample chamber. The microscope was operated at an accelerating voltage of 5.0 kV.

2.3.4. Energy dispersive x-ray spectroscopy (EDS)

Elemental analysis of the SiO_2 particles and MSiO_2 particles were performed by EDS spectra. For EDS analysis, the sample was taken into a vial and dried at the oven.

Platinum was sputtered on the sample to ensure the conductivity of the sample surface. The sample is then mounted to a sample chamber. The microscope was operated at an accelerating voltage of 5.0 kV.

2.3.5. Mechanical properties analysis for elongation

Hydrogels with dimension of 2mm thick and 10 mm length were used for uniaxial tensile measurement. The tensile measurement was conducted by universal testing machine (UTM) at ambient temperature. The crosshead speed was 50mm/min. The stress and strain curves were recorded using the machine. The stress (σ) was calculated according to the equation,

$$\sigma = F/\pi r^2$$

Where, F is the recorded load and r is the original radius of the specimen. The strain (ε) was calculated from the change of the length (l) to the initial gauge length (l_0) of the measured sample, and was calculated by the equation,

$$\varepsilon = l/l_0 \times 100$$

The initial modulus was calculated as the initial slope of the stress-strain curve. The fracture toughness was calculated by integrating the area of the stress-strain curve of each sample.

2.3.6 The compressive stress–strain measurements

The compressive measurements of the hydrogels were conducted on a UTM at ambient temperature. The crosshead speed was 50mm/min. Each specimen was tested at least three times to check the reproducibility. The cylindrical hydrogel samples were cut into 10-15 mm in diameter and 4–8 mm in thickness.

2.3.7 Transmittance spectra

The transmittance of the prepared hydrogels was measured using an ultraviolet-visible light. We used UV-Vis curing machine (Ocean Optics Spectrometers) in the range of wavelength 200nm to 800nm at 25°C. Such equipment allows measuring solid or soft materials such as hydrogels. The hydrogel samples were 2.0 mm thickness which was

placed into the glass surface between the two perpendicular UV-Vis light source. Spectrum of transmittance as a function of wavelength was obtained only in the ultra violet and visible region.

2.4 References

- [1] D. Schumacher, M. Wilhelm, and K. Rezwani, "Modified solution based freeze casting process of polysiloxanes to adjust pore morphology and surface functions of SiOC monoliths," *Mater. Des.*, vol.160, pp.1295-1304 (2018).
- [2] J. Jiang, W. Wang, H. Shen, J. Wang, and J. Cao, "Characterization of silica particles modified with γ -methacryloxypropyltrimethoxysilane," *Appl. Surf. Sci.*, vol. 397, pp. 104-111 (2017).
- [3] H. Ghasemzadeh and F. Ghanaat, "Antimicrobial alginate/PVA silver nanocomposite hydrogel, synthesis and characterization," *J. Polym. Res.*, vol. 21, pp.1-14 (2014).
- [4] J. Fan, Z. Shi, M. Lian, H. Li, and J. Yin, "Mechanically strong graphene oxide/sodium alginate/polyacrylamide nanocomposite hydrogel with improved dye adsorption capacity," *J. Mater. Chem. A*, vol.1, pp. 7433-7443 (2013).

Chapter 3

Results and Discussion

3.1 Synthesis of AAm-MSiO₂ nanocomposite hydrogel

Nanocomposite hydrogels are synthesized at room temperature by free radical polymerization of AAm with the KPS as an initiator, TEMED as an accelerator and MSiO₂ particles as cross-linker [1-2]. AAm, MSiO₂, TEMED and water were taken in a vial and continuously stirred until the well dispersion of MSiO₂. In another container, 2.96 mM KPS solution in water was prepared. Then both solutions were transferred into a separate test tube for nitrogen gas bubbling for 30 minutes to remove any dissolved oxygen. After N₂ bubbling, KPS was added into the solution of gel precursors in an ice bath. Polymerization was carried out for 24 h at room temperature to obtain a nanocomposite (NC) hydrogel. Fig.3.1.is the pictorial representation of a polymer network into the NC gel.

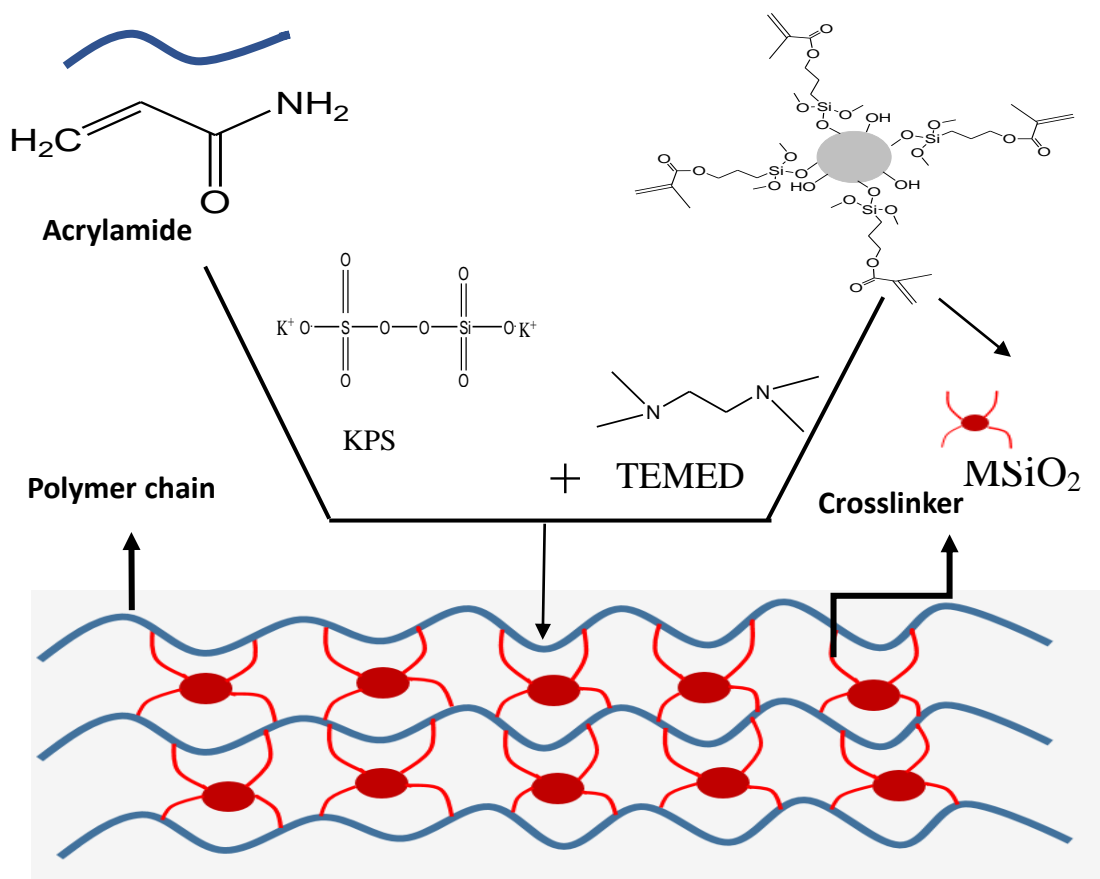
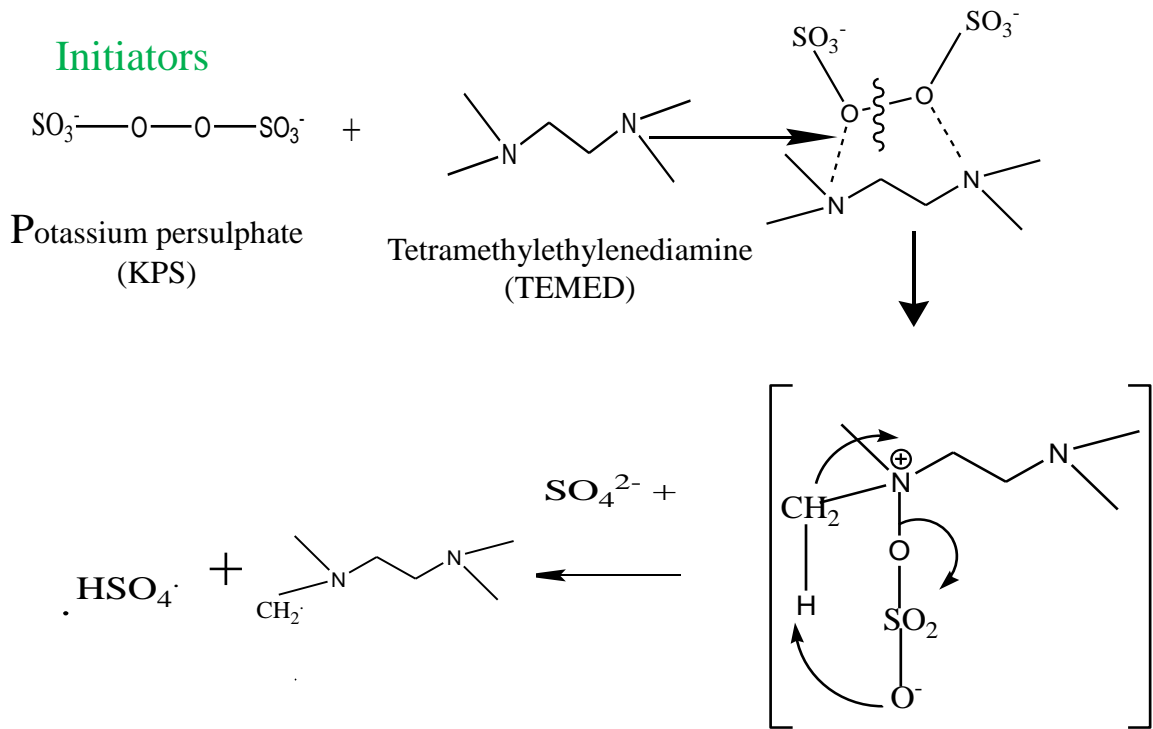


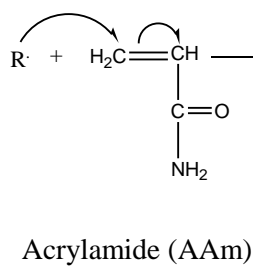
Fig. 3. 1: AAm-MSiO₂ nanocomposite hydrogel

3.2 Mechanism of free radical polymerization of AAm

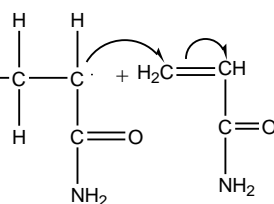
Initiators



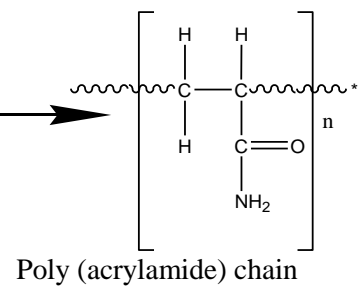
Initiation



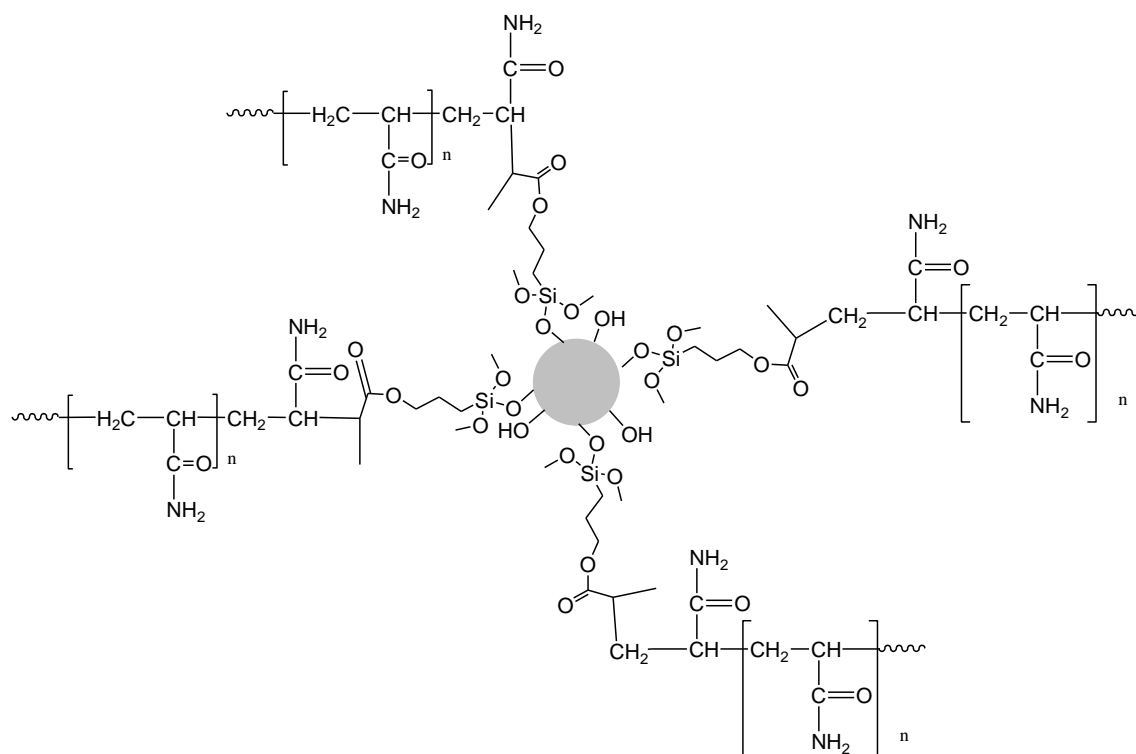
Propagation



Termination

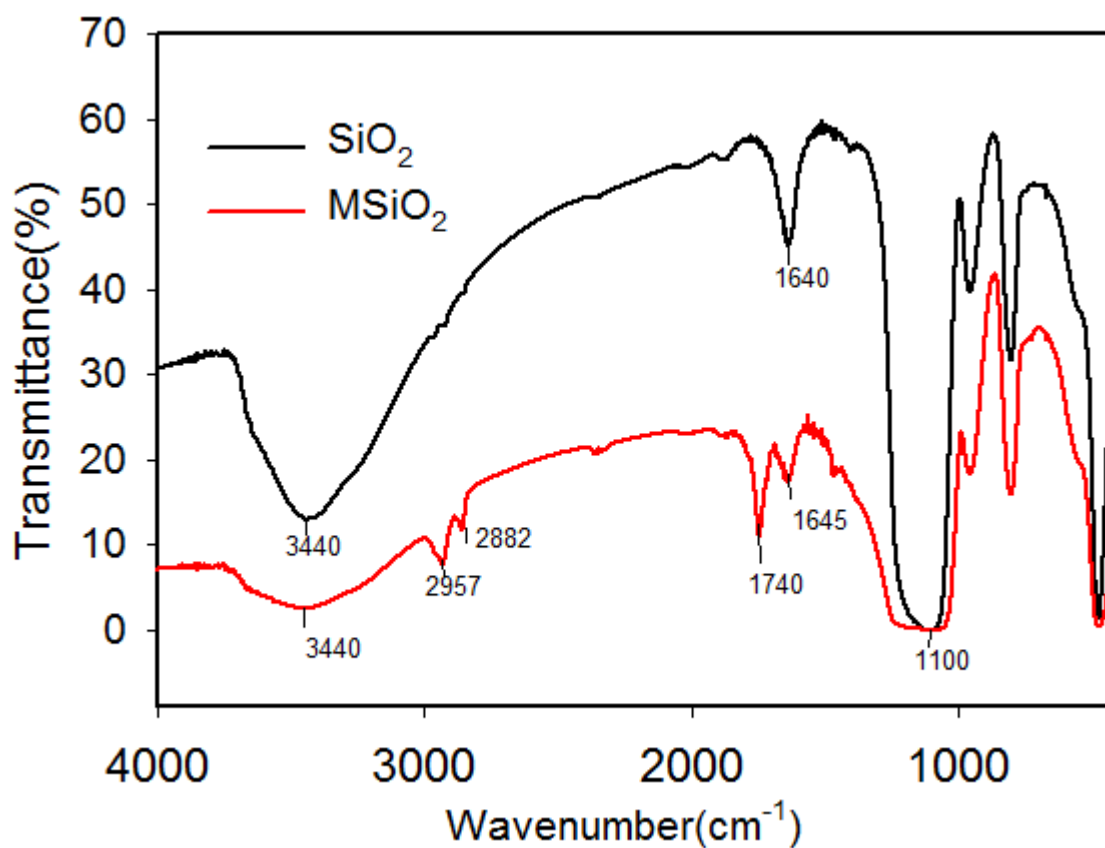


3.2.1 Proposed chemical structure of AAm-MSiO₂ hydrogel



3.3 Functional Group investigation by Fourier Transform Infrared (FT-IR) Spectroscopy

The FT-IR spectra of pure SiO₂ and MSiO₂ are shown in Fig. 3.2. After modification with MPTS, the additional peak of C=O, C=C appears in MSiO₂. The peak at 1100 cm⁻¹ is ascribed to stretching vibration of Si-O-Si, the peak at 950 cm⁻¹ is assigned to Si-OH, the peak at 802 cm⁻¹ is due to stretching vibration of Si-O, and the peak at 470 cm⁻¹ belongs to vibration of Si-O groups. In MSiO₂, a carboxyl group (C=O) at 1740 cm⁻¹, and also peaks at 2957, 2882, and 1645 cm⁻¹ which are assigned to C-H (-CH₃) stretching, C-H (-CH₂) stretching, and C=C stretching vibration, respectively are observed. It indicates that MPTS was successfully grafted onto the surface of silica nanoparticles [3]. The appearance of -OH peaks for MSiO₂ indicating that there are still a number of unreacted -OH groups at the surface of MSiO₂.

Fig. 3. 2: FT-IR spectra of bare SiO₂ and MSiO₂Table 3. 1: Characteristic peaks of SiO₂ and MSiO₂

Wave number (cm ⁻¹)	Interpretation
3440	O-H (Si-OH) stretching
2952	C-H (-CH ₃) asymmetric stretching
2857	C-H(-CH ₂) symmetric stretching
1740	C=O Stretching
1640	C=C Stretching
1100	Si-O-Si stretching

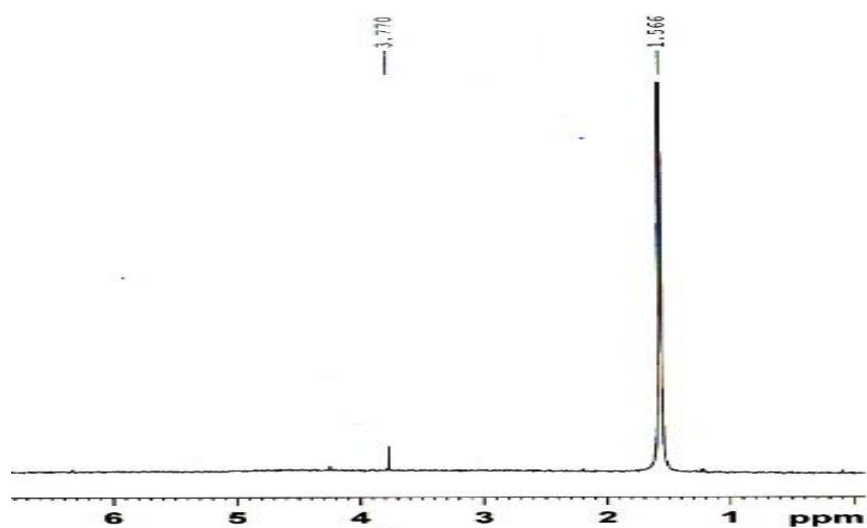
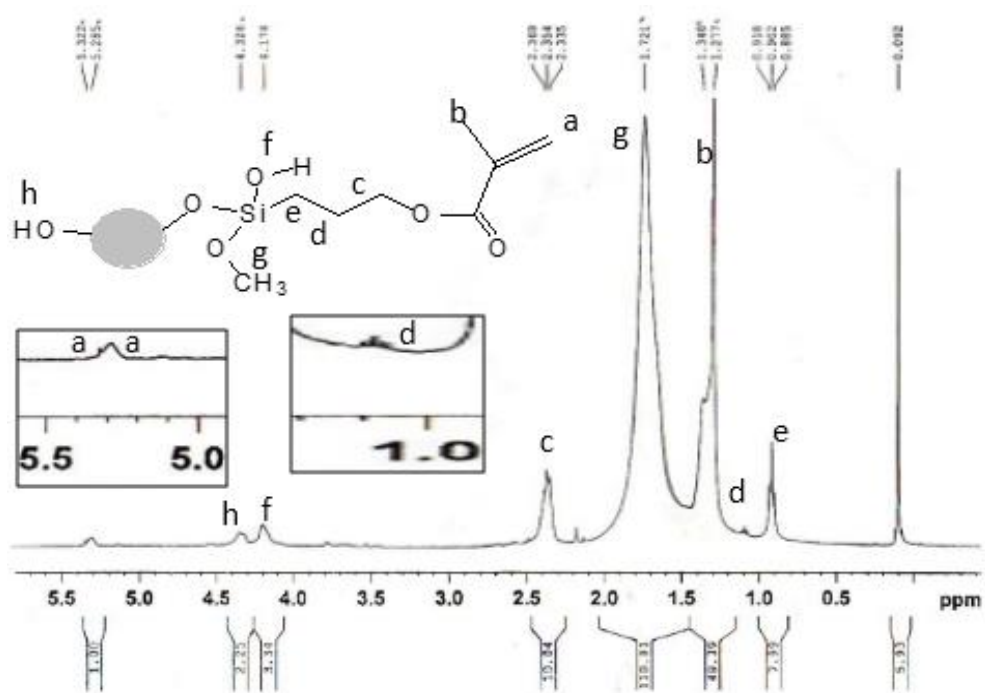
Fig. 3. 3: $^1\text{H-NMR}$ spectra of bare SiO_2 Fig. 3. 4: $^1\text{H-NMR}$ spectra of MSiO_2

Table 3. 2: $^1\text{H-NMR}$ data for MSiO_2

Chemical shift	Number of photons
5.28	a 1H singlet
5.32	a 1H singlet
2.33-2.36	c 2H triplet
1.05-1.1	d 4H pentate
0.883-0.91	e 2H triplet
1.27	b 1H singlet
1.72	g 1H singlet
4.1	f 1H singlet
4.32	h 1H singlet

3.4 Study of surface morphology SiO_2 (300nm) and MSiO_2 (300nm)

The surface morphology of bare SiO_2 and MSiO_2 (300nm) particles were studied by FE-SEM. The bare SiO_2 and MSiO_2 surface are shown in Fig. 3.5(A), and MSiO_2 3.5(B) with magnification $\times 50,000$. It is observed that the particles both for SiO_2 and MSiO_2 are homogeneously spherical in shape. The size of SiO_2 is ranging from 295nm to 315nm and average particle size is 302.5nm. The size of MSiO_2 is ranging from 300 nm to 318nm and average particle size 311.5nm. The polydispersity of SiO_2 and MSiO_2 is very low. The particle sizes are slightly increased from bare SiO_2 to MSiO_2

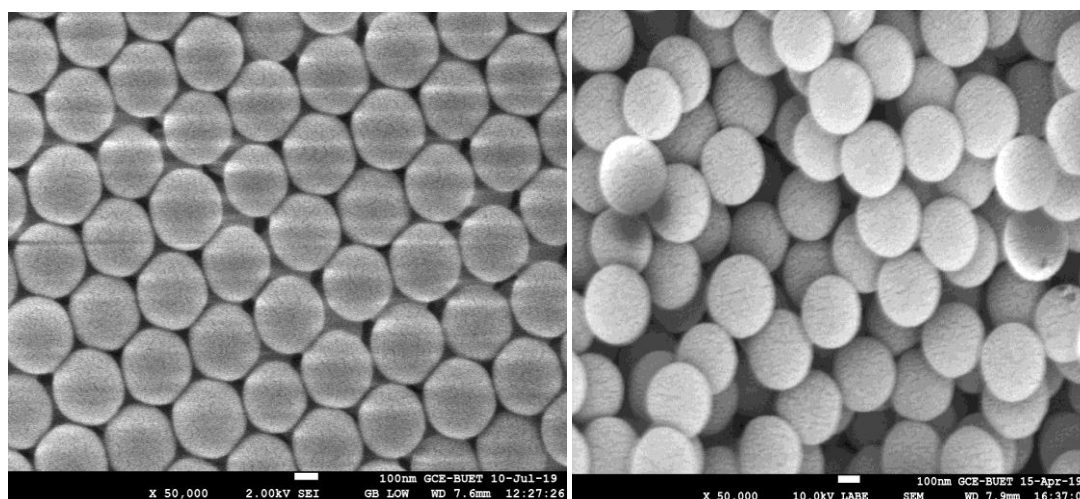


Fig. 3. 5 : SEM image of a) bare SiO₂ (300nm) with magnification×50,000 and b) MSiO₂ (300nm) with magnification ×50,000

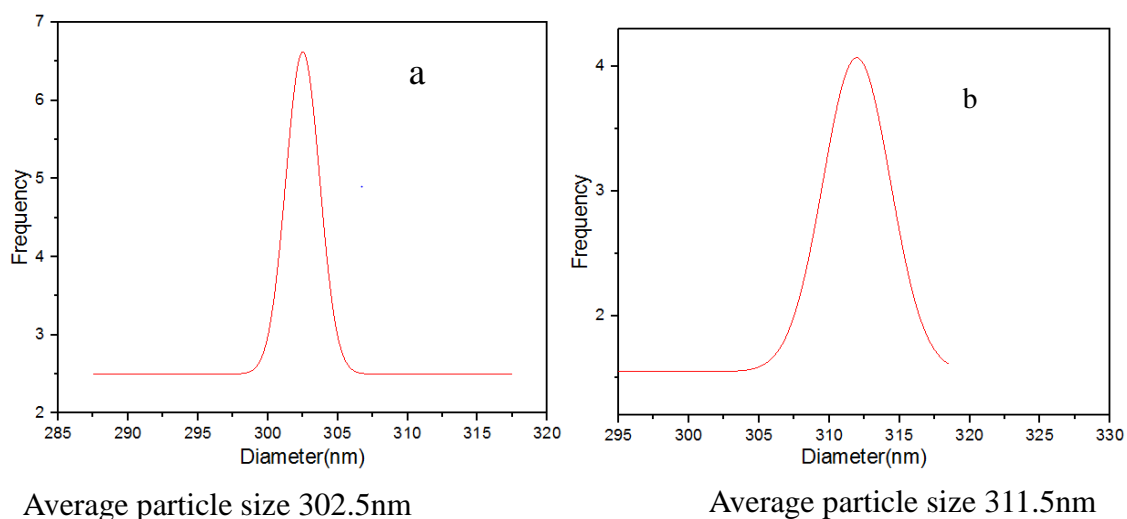


Fig. 3. 6 : Particle size distribution curve of Silica(302.5nm) and MSiO₂ (311.5nm) using imageJ software

3.5 Study of surface morphology SiO₂ (200nm) and MSiO₂ (200nm)

The Morphology and particle size of SiO₂ and MSiO₂ for 200nm were done through SEM analysis (figure 3.7). The particles are spherical in shape both for SiO₂ and MSiO₂. After vinyl modification, the particles remained spherical and their size was slightly increased. Surface modification with vinyl groups did not induce significant changes in the particle size distribution.

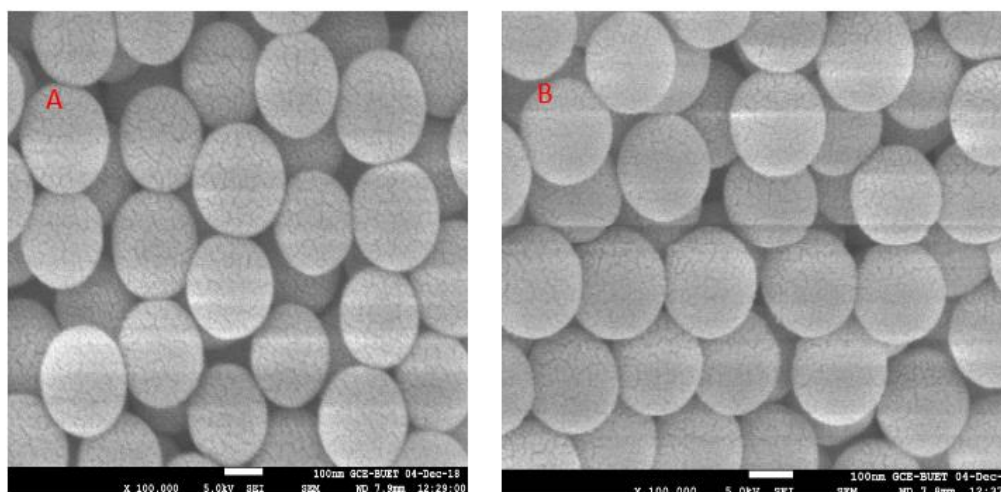


Fig. 3. 7 : SEM image of a) bare SiO₂ (200nm) with magnification×100,000 and b) MSiO₂ (200nm) with magnification ×100,000

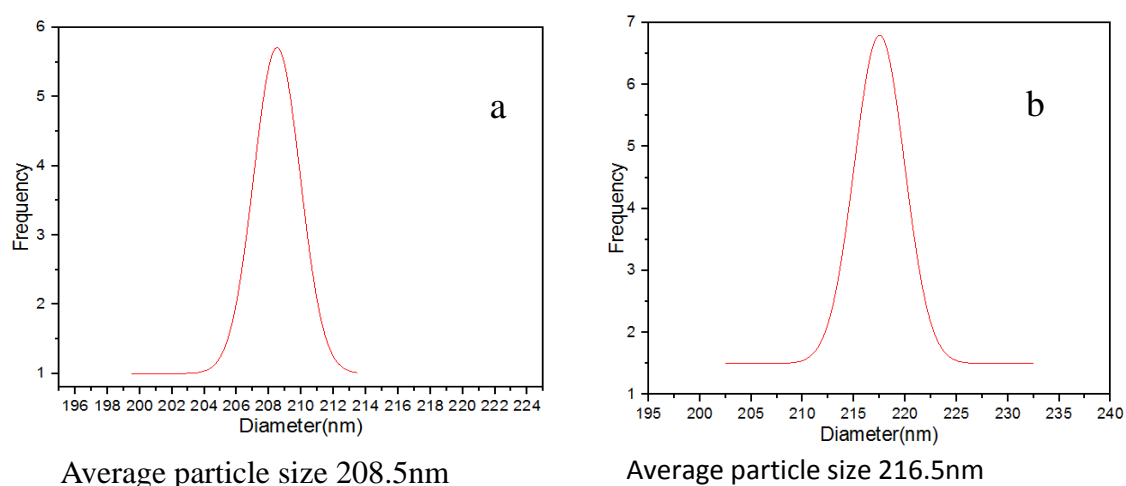


Fig. 3. 8 : Particle size distribution curve of SiO₂ (208.5nm) and MSiO₂ (216.5nm) using imageJ software

3.6. Study of surface morphology MSiO₂ (100nm)

The surface morphology of MSiO₂ (100nm) particle was studied by FE-SEM. The modification of silica surface is shown in Fig. 3.9(A), 3.9(B) at different magnifications. It is observed that the particles are spherical in shape. The particle size is ranging 100 nm to 120 nm and the average particle size is 117.5nm. The polydispersity of SiO₂ and MSiO₂ is very low.

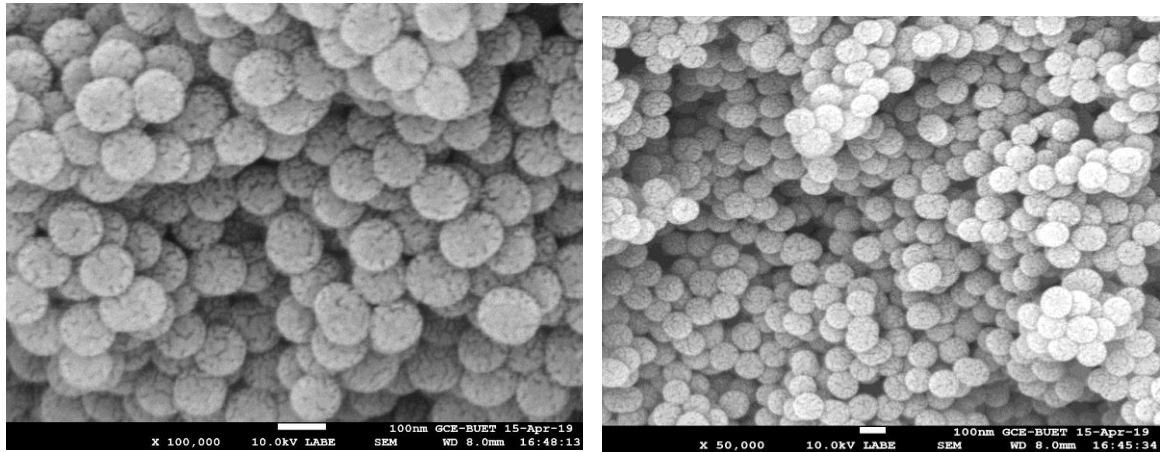
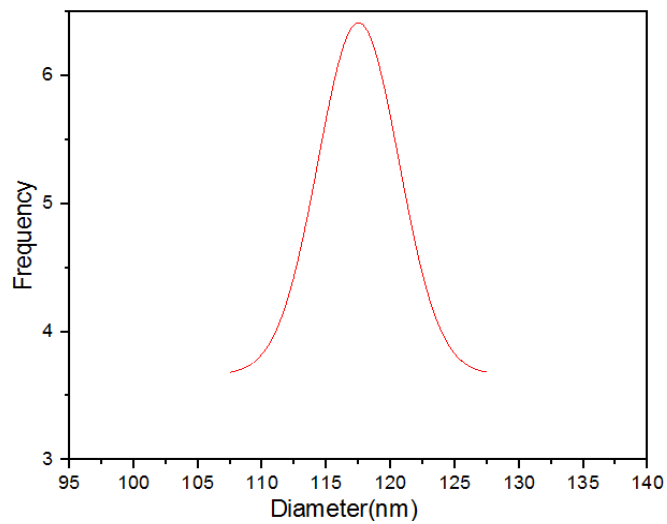


Fig. 3. 9 : SEM image for a) MSiO₂ (100 nm) with magnification×100,000 and b) magnification ×50,000



Average particle size is 117.5nm

Fig. 3. 10 : Particle size distribution curve of MSiO₂ (117.5nm) using imageJ software

3.7 EDS analysis of MSiO₂ (300nm)

Table 3.3 shows that the mass percentage of C, O and Si in MSiO₂ (300nm) is 8.47%, 55.51% and 36.02 % and the atom percentage is 12.93%, 63.57% and 23.50%, respectively.

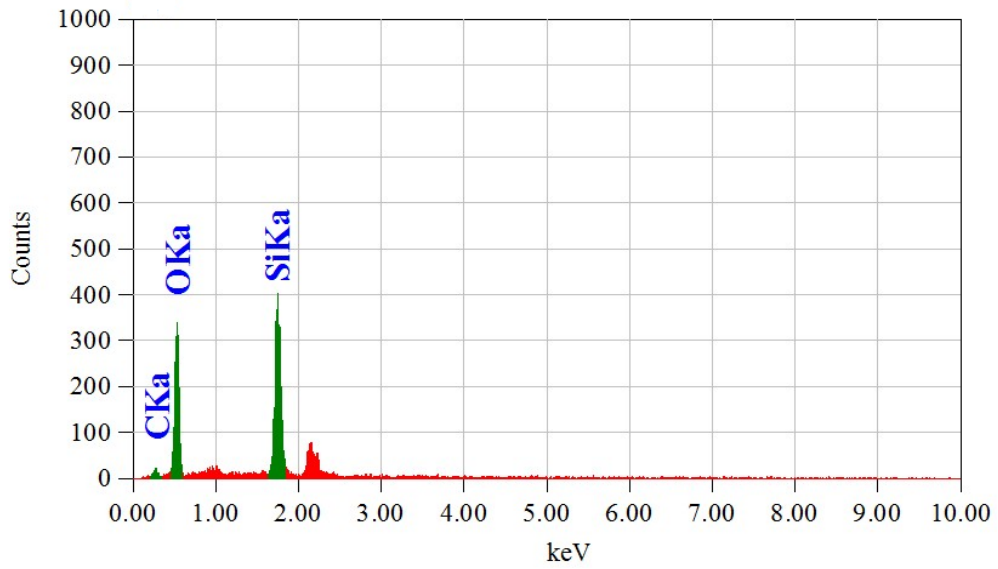


Fig. 3. 11: EDS spectra of MSiO₂ (300 nm)

Table 3. 3: EDS spectra of MSiO₂ (300nm)

Element	(KeV)	mass %	atom %
C	0.277	8.47	12.93
O	0.525	55.51	63.57
Si	1.739	36.02	23.50

3.8 EDS analysis of SiO₂ (200nm)

Table 3.4 reveals that the mass percentage of O and Si in SiO₂ (200 nm) is 48.60%, 51.40% and the atom percentage is 59.98% and 40.02 %, respectively.

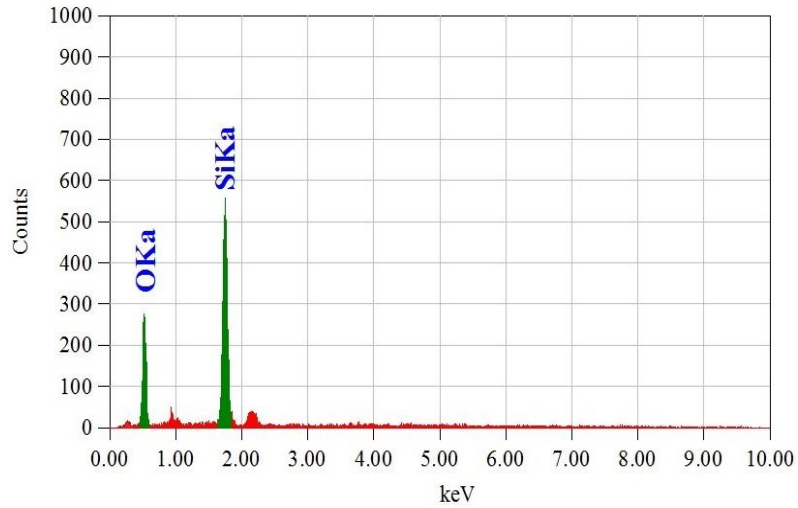


Fig. 3. 12: EDS spectra of bare SiO₂ (200nm)

Table 3. 4 : EDS spectra of bare SiO₂ (200nm)

Element	(KeV)	mass %	atom %
O	0.525	48.60	59.98
Si	1.739	51.40	40.02

3.9 EDS analysis of MSiO₂ (200nm)

Table 3.5 reveals that the mass percentage of C, O and Si in MSiO₂ (200nm) is 16.00%, 48.87% and 35.13% and the atom percentage is 18.1%, 55.5%, and 26.4 %, respectively.

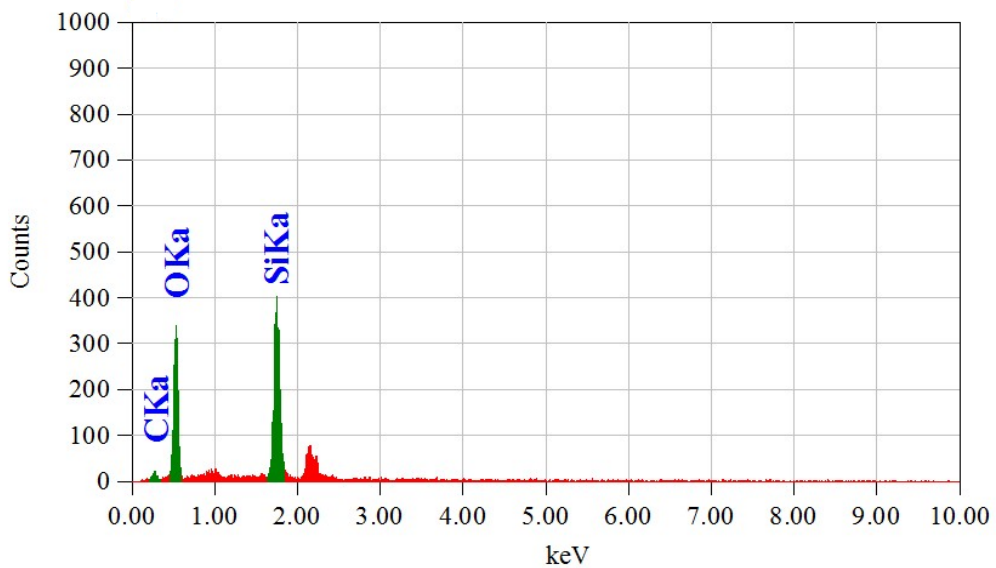


Fig. 3. 13: EDS spectra of MSiO₂ (200nm)

Table 3. 5: EDS spectra of MSiO₂ (200nm)

Element	(KeV)	mass %	atom %
C	0.277	16.00	18.1
O	0.525	48.87	55.5
Si	1.739	35.13	26.4

3.10 EDS spectra of MSiO₂ (100 nm)

Table 3.6 reveals that the atom percentage of C, O and Si in MSiO₂ (100 nm) is 10.96%, 65.62% and 23.42% and the mass percentage is 7.16%, 57.08%, and 35.36 %, respectively.

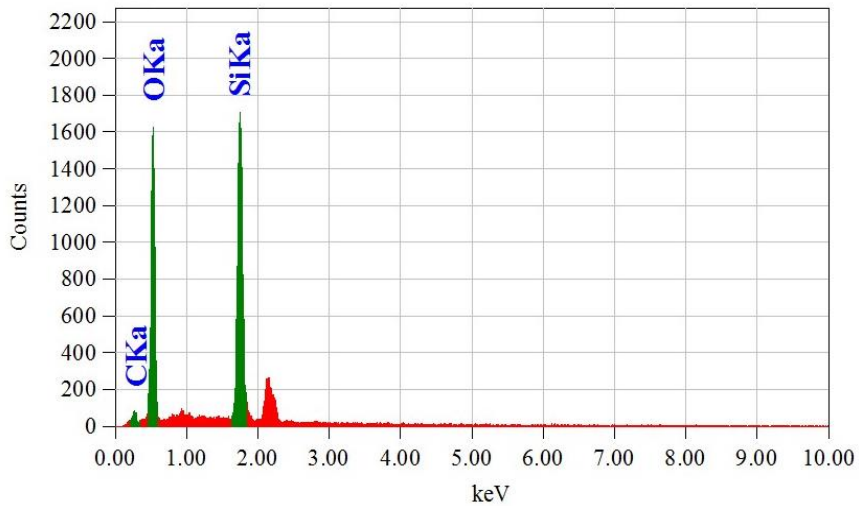


Fig. 3. 14: EDS spectra of MSiO₂ (100nm)

Table 3. 6: EDS spectra of MSiO₂ (100 nm)

Element	(KeV)	mass %	atom %
C	0.277	7.16	10.96
O	0.525	57.08	65.62
Si	1.739	35.36	23.42

3.11 Transmittance spectra of synthesized hydrogels

Transparency is a significant feature of the polymeric hydrogels to know about the crosslinking network. Therefore, it is crucial to investigate transparency of AAm-MSiO₂ nanocomposite hydrogels. All the hydrogels are highly transparent throughout the visible region of light. It indicates the formation of homogeneous network structure in the polymer matrix. In addition, the transparency of the prepared hydrogels increases with decreasing amount of MSiO₂ where the diameter of the hydrogel is fixed. A₄S_{0.50%} hydrogel shows more than 90% transmittance on the other hand the transmittance of A₄S_{1.25%} hydrogel decreases to more than 75%.

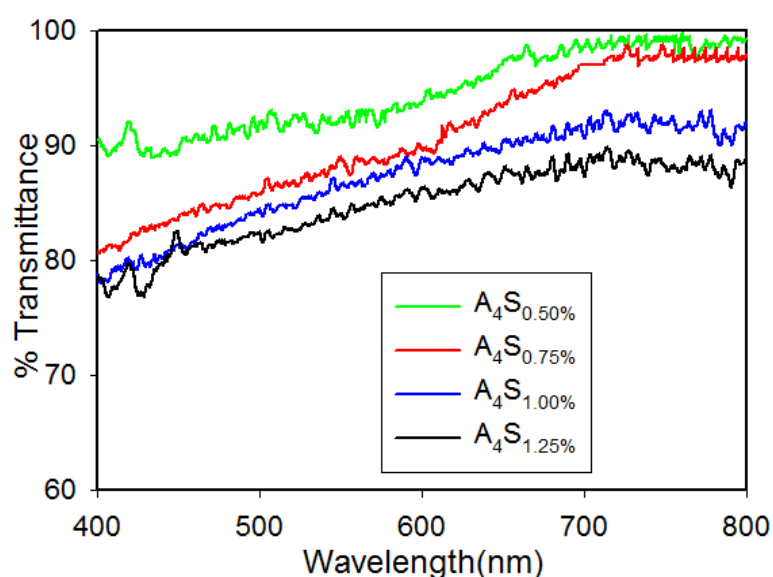


Fig. 3. 15: Transmittance spectra of AAm-MSiO₂ hydrogels



Fig. 3. 16: Photograph of highly transparent AAm-MSiO₂ hydrogels

3.12.1 Tensile test of AAm -BIS hydrogels

The mechanical properties of conventional AAm-BIS hydrogels have been studied

under uniaxial tension. Fig 3.17 represents the stress -strain curves of AAm-BIS hydrogel prepared by varying concentration of BIS and AAm monomer. All the prepared hydrogels can be elongated only 100% strain to maximum 160% strain. The concentration of crosslinker is the important factor for the mechanical properties of the hydrogel. It is clearly seen that the increasing BIS concentration from 20mM to 100 mM significantly increases the mechanical properties (toughness, tensile strength, and young's modulus). The formation of more covalent bonds with the polymer chains and crosslinkers gives the tough network structure in the hydrogel. Generally, the increase of crosslinking density decreases the gels flexibility (percentage elongation at break) and the hydrogel becomes more brittle. The elongations at break of AAm-BIS hydrogels are completely dependent on BIS and AAm concentration. At constant AAm and water content, the elongations at break for AAm-BIS (A_2B_{100}) hydrogel was found the lowest than others. As expected, Young's moduli of hydrogel increased linearly with increasing BIS concentration. The mechanical properties of hydrogels initially increase with the increase crosslinker concentration. However, above a threshold crosslinker concentration, the mechanical properties for each hydrogel reach to a plateau value.

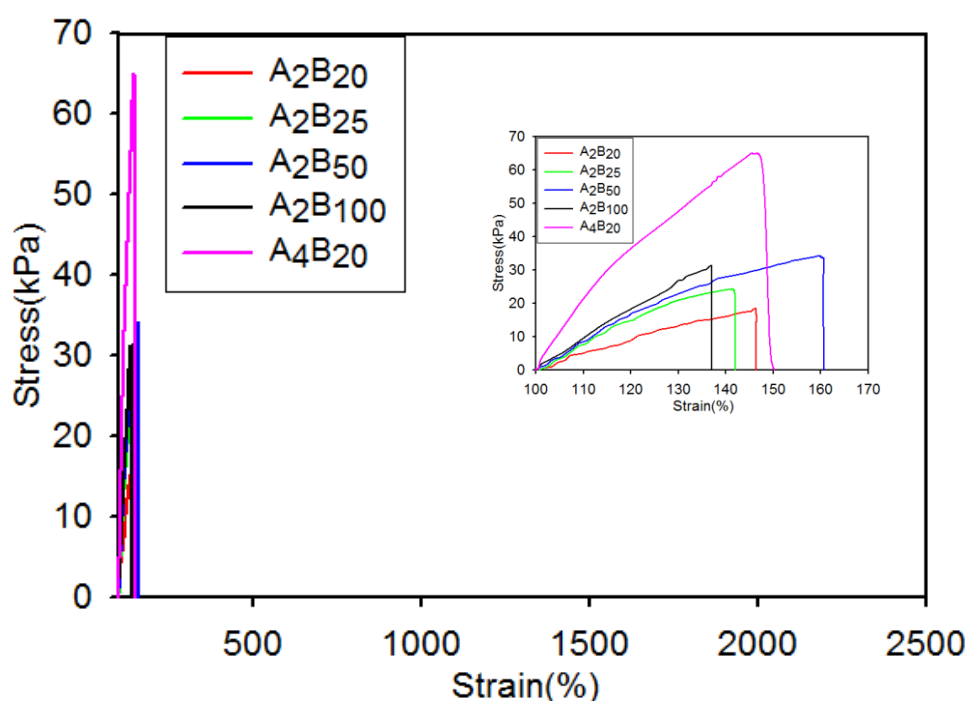


Fig. 3. 17: Stress –strain curves of AAm-BIS hydrogels prepared by varying concentration of BIS under uniaxial tension

Table 3. 7: Table for tensile properties of AAm-BIS hydrogels prepared by varying concentration of BIS

Sample code	Toughness (kJ/m ³)	Tensile Strength (KPa)	Young Modulus (KPa)	Elongation at break (%)
A ₂ B ₂₀	46	18	0.44	144
A ₂ B ₂₅	60	23	0.78	142
A ₂ B ₅₀	125	38	0.81	162
A ₂ B ₁₀₀	61	31	0.91	138
A ₄ B ₂₀	20	65	2.12	150

3.12.2 Comparison of tensile test of AAm-MSiO₂ (216.5 nm) and AAm-BIS hydrogels

AAm-MSiO₂ and AAm-BIS hydrogels are differed markedly with regard to their mechanical properties during elongation. Typical strain–stress curves for different weight (%) of crosslinker are given in Fig. 3.18. The tensile strength and young modulus of AAm-MSiO₂ are low compared with the mechanically toughened AAm-BIS. But AAm-BIS hydrogels readily break at lower applied stress during elongation and its elongation at break are found in the range of 135% to 160%. The AAm-BIS hydrogels are brittle in nature because the bifunctional BIS crosslinker reduces the polymer chain length into the polymer network. On the other hand, AAm-MSiO₂ hydrogel exhibit rubber-like behavior. Elongations of AAm-MSiO₂ hydrogels are much higher and shows 2400% of strain without any break. The physical and covalent interaction between the polymer chain and well dispersed crosslinker MSiO₂ into the

polymer network gives the polymer chains much freedom to dissipate energy under applied stress. Tensile strength, young modulus and toughness of AAm-MSiO₂ hydrogels change with increasing MSiO₂ content. At constant MSiO₂, the tensile strength, young modulus and toughness increases with the increase of AAm concentration. The tensile properties of AAm-BIS hydrogel also dependent on the AAm concentration.

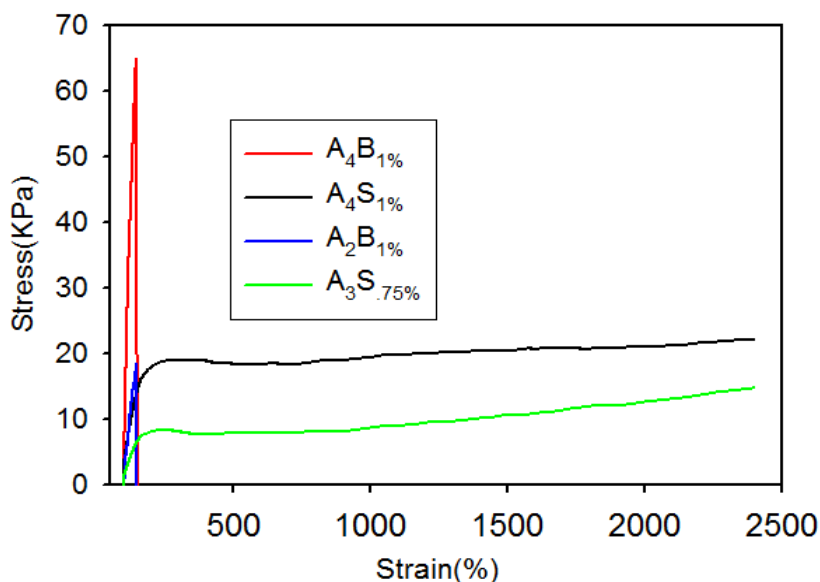


Fig. 3. 18 : Stress –strain curves of AAm-MSiO₂ and AAm-BIS hydrogels prepared by varying concentration of BIS and MSiO₂ under uniaxial tension.

Table 3. 8 : Tensile properties of AAm-MSiO₂ and AAm-BIS hydrogels

Sample code	Toughness (kJ/m ³)	Tensile Strength (KPa)	Young Modulus (KPa)	Elongation at break (%)
A ₄ B ₁ %	203	65.00	2.12	150
A ₄ S ₁ %	453	20.99	0.24	No break
A ₂ B ₁ %	41	18.00	0.44	144
A ₃ S _{.75} %	231	11.20	0.11	No break

3.12.3 Compressive strength of AAm -BIS hydrogels

With increasing cross-linker amount leads to the enhancement in the compressive strength. Distinct from stretching, the network becomes gradually denser as the extent

of compression is increased, the increase of network crosslinking density generally decreases the gels flexibility. From Fig. 3.19, it is observed that the breaking strains decrease with an increment of monomer concentration and crosslinker concentration due to the increased covalent bonding density. AAm (4M) hydrogel show less stretchability than AAm (2M) hydrogel due to the presence of more cross-linking with the polymer chains. With increasing BIS amount, the deformation is decreased while the modulus is increased, indicating the increase in cross-linking density and a decrease in the length of the polymer chains between the cross-linking points.

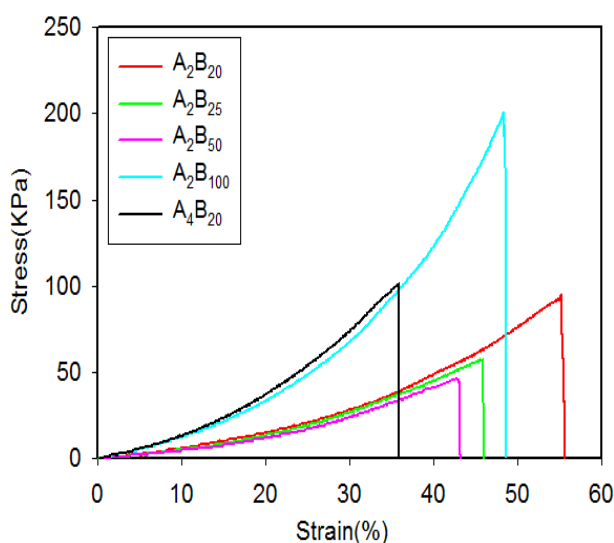


Fig. 3. 19: Stress –strain curves of AAm-BIS hydrogels prepared by varying concentration of BIS under uniaxial compression.

Table 3. 9 :Table for compressive properties of AAm-BIS hydrogels prepared by varying concentration of BIS

Sample code	BIS (mM)	Toughness (kJ/m ³)	Compressive Strength (KPa)	Young Modulus (KPa)	Compression at break (%)
A ₂ B ₂₀	20	18	45	0.83	55
A ₂ B ₂₅	25	10	57	0.66	48
A ₂ B ₅₀	50	8	93	0.65	45
A ₂ B ₁₀₀	100	31	200	1.67	49
A ₄ B ₂₀	20	14	101	1.63	35

3.12.4 Comparison of compressive strength of AAm-BIS and AAm-MSiO₂ hydrogels

AAm-MSiO₂ hydrogels and AAm-BIS hydrogels are remarkably differed with regard to their compressive strength. Typical strain–stress curves for different weight (%) of crosslinker are given in Fig. 3.20. It is clearly observed that AAm-BIS hydrogels readily break at lower deformation by applying force and its break are in the range of 38% to 45%. On the other hand, AAm-MSiO₂ hydrogel does not break but it deformed in the range of 65% to 75%. The AAm-BIS hydrogels are brittle in nature, but AAm-MSiO₂ hydrogel exhibit soft and rubber-like behavior. The young modulus and toughness of AAm-BIS hydrogels are much higher than the AAm-MSiO₂ hydrogels.

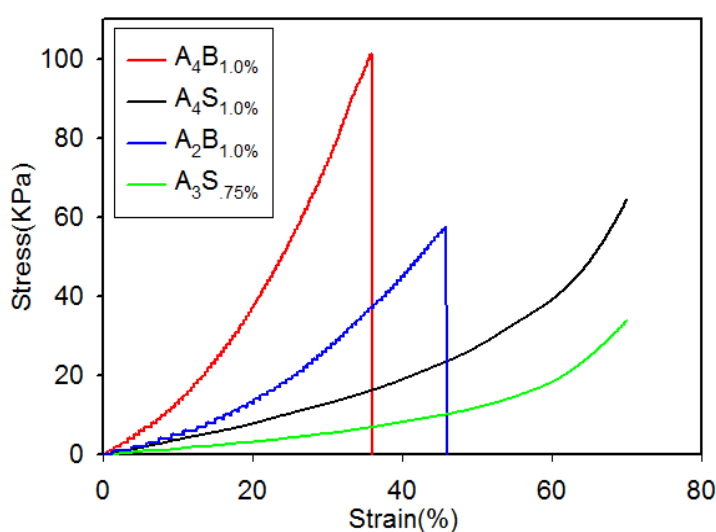


Fig. 3. 20 : Stress –strain curves of AAm-MSiO₂ and AAm-BIS hydrogels prepared by varying concentration of BIS and MSiO₂ under uniaxial compression.

Table 3. 10 :Compressive strength of AAm-MSiO₂ and AAm-BIS hydrogels prepared by varying concentration of BIS and MSiO₂

Sample code	Toughness (kJ/m ³)	Compressive Strength (KPa)	Young Modulus (KPa)	Compression at break (%)
A ₄ B _{1%}	14	101	1.63	38
A ₄ S _{1%}	14	65	0.46	No break
A ₂ B _{1%}	10	57	0.66	45
A ₃ S _{.75%}	9	26	0.11	No break

3.12.5 Tensile test of AAm-MSiO₂-BIS (A₂S_{Y%}B_{0.7}) hydrogels

The AAm-MSiO₂ hydrogels prepared using lower concentration of AAm gives highly sticky hydrogels which strongly adhere on the glass surface. It can be overcome using slight amount of conventional crosslinker BIS besides MSiO₂. Typical strain–stress curves for different weight (%) of crosslinker MSiO₂ at constant AAm and BIS concentration are given in Fig. 3.21. A direct correlation of the MSiO₂ weight (%) and the mechanical properties of the hybrid hydrogels is observed. A₂S_{1.50%}B_{0.7} hydrogel exhibits the highest tensile strength with an average stress at break 32 KPa. A₂S_{1.50%}B_{0.7} hydrogel can be elongated up to 706% whereas A₂S_{0.75%}B_{0.7} can be extended up to 1062% with average stress at break of 30 KPa. The higher MSiO₂ concentration results in stiff gels with higher ultimate tensile strength, but lower elongation at break.

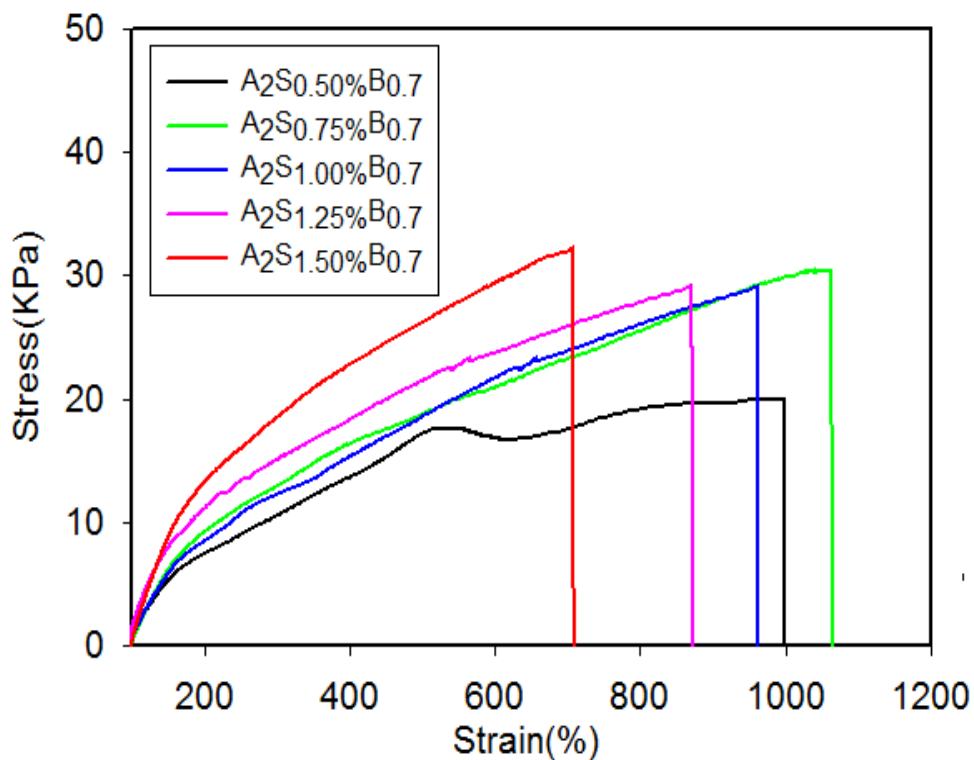


Fig. 3. 21: Stress –strain curves of AAm-MSiO₂-BIS hydrogels prepared by varying concentration of BIS and MSiO₂ under uniaxial tension.

Table 3. 11 : Table for tensile properties of AAm-MSiO₂-BIS (A₂S_YB.7) hydrogels

Sample code	Toughness (kJ/m ³)	Tensile Strength (KPa)	Young Modulus (KPa)	Elongation at break (%)
A ₂ S _{0.50%} B.7	134	20	0.090	999
A ₂ S _{0.75%} B.7	191	30	0.096	1062
A ₂ S _{1.00%} B.7	159	29	0.10	960
A ₂ S _{1.25%} B.7	152	29	0.13	869
A ₂ S _{1.50%} B.7	131	32	0.16	706

3.12.6 Tensile test of AAm -MSiO₂ (216.5 nm) hydrogels with varying concentration MSiO₂

Typical stress- strain curves for different weight (%) of the crosslinker is given in Fig. 3.22. The amount crosslinker (%) into the hydrogel plays an important role in determining the mechanical properties of hydrogels. The greater weight (%) of crosslinker generally leads to a stronger and harder hydrogel [4]. Results derived from stress-strain measurements, as depicted in Table 3.12, shows that an increase in the crosslinker (%) results increase tensile strength, Young's modulus and toughness as more interaction between MSiO₂ and AAm chains are occurred. The most important things that all the hydrogels are highly stretchable and do not break in the region of strain up to 2400%. The hydrogel shows extraordinary extensibility that could reach 24 times from the original length without any break. Thus, when MSiO₂ content decreases; the final material is become very soft with poor mechanical properties (lower modulus, tensile strength, and toughness). This clearly indicates that the degree of crosslinking in the network play a major role in the mechanical properties of the hydrogel. The extent of crosslinking in the network is proportional to the tensile strength, Young's modulus, and toughness (Fig.3.22) of hydrogels.

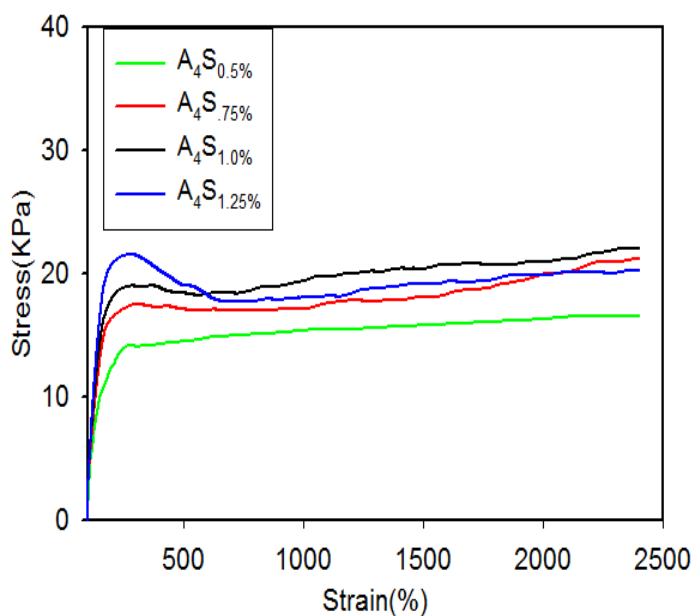


Fig. 3. 22 : Stress –strain curves of AAm-MSiO₂ (216.5nm) hydrogels prepared by varying concentration of MSiO₂ under uniaxial tension.

Table 3. 12 : Table for tensile properties of AAm-MSiO₂ (216.5nm) hydrogels prepared by varying concentration of MSiO₂

Sample code	Toughness (kJ/m ³)	Tensile Strength (KPa)	Young Modulus (KPa)	Elongation at break (%)
A ₄ S _{0.5%}	350	17	0.18	No break
A ₄ S _{0.75%}	415	19	0.22	No break
A ₄ S _{1.00%}	453	21	0.24	No break
A ₄ S _{1.25%}	437	22	0.28	No break

3.12.7 Compressive strength of AAm-MSiO₂ (216.5nm) hydrogels prepared by varying concentration of MSiO₂

The compressive strength of AAm-MSiO₂ (216.5nm) hydrogels is substantially enhanced by the addition of MSiO₂ as a crosslinker. AAM-MSiO₂ hydrogels with high MSiO₂ content possess higher strength due to strong attraction between the polymer and MSiO₂ particles [5]. Hence, when the MSiO₂ content in the formulation increased, the hydrogel fraction increased, leading to an increase in the compression strength, toughness and young modulus (table 3.13).

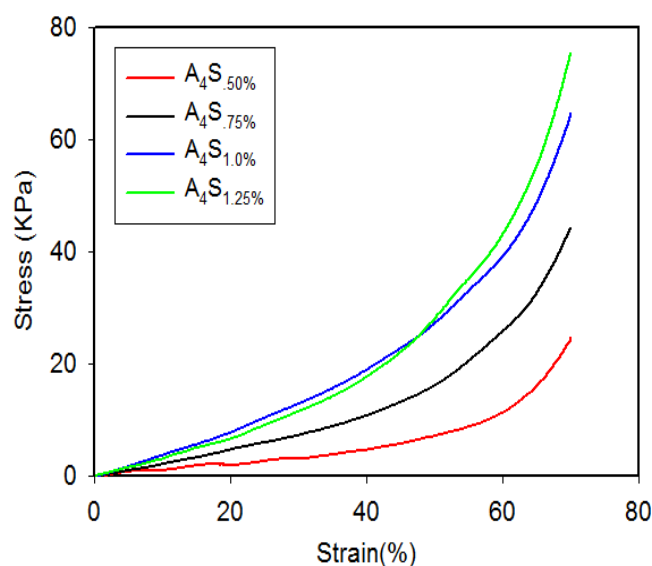


Fig. 3. 22 : Stress –strain curves of AAm-MSiO₂ (216.5 nm) hydrogels prepared by varying concentration of MSiO₂ under uniaxial compression.

Table 3. 13: Compressive properties of AAm-MSiO₂ (216.5 nm) hydrogels prepared by varying concentration of MSiO₂

Sample code	Toughness (kJ/m ³)	Compressive Strength (KPa)	Young Modulus (KPa)
A ₄ S _{.05%}	4	25	0.10
A ₄ S _{.75%}	9	44	0.25
A ₄ S _{1.00%}	14	65	0.46
A ₄ S _{1.25%}	15	75	0.44

3.12.8 Tensile test of different AAm-MSiO₂ ((117.5nm, 216.5nm and 311.5nm) hydrogels prepared by varying concentration of AAm

The AAm concentration also has a great effect on the mechanical property of AAm-MSiO₂ hydrogel [6]. The mechanical property (toughness, tensile strength, and young modulus) significantly increases with increasing AAm concentration under the constant weight (%) of MSiO₂. When the concentration of AAm increases, the entanglement of the polymer chains and the interaction between the AAm chain and MSiO₂ crosslinker are also increased. Fig.3.24 represents the AAm-MSiO₂ hydrogel where average silica particle size was 117.5nm. The AAm-MSiO₂ hydrogel for the 3M AAm concentration, the interaction between MSiO₂ crosslinker and AAm chain is less than 4M AAm hydrogel. As a result, it shows lower mechanical properties than the 4M hydrogels. But for the 5M AAm concentration, the exceptional mechanical properties is appeared. It starts to decrease the stress after reaching to a certain point of stress. But for the other two hydrogels, the stress gradually increases after the yield point in the plastic region. The main difference observed among these three hydrogels is in the elastic region. Regardless of the direction in which the hydrogel is elongated, the hydrogel showed extraordinary extensibility that could reach 24 times from the original length without break. The stress-strain measurements cannot be proceeded further due to instrument limitation. The toughness, young's modulus, tensile strength data of the hydrogels are given in Table 3.14 and 3.15

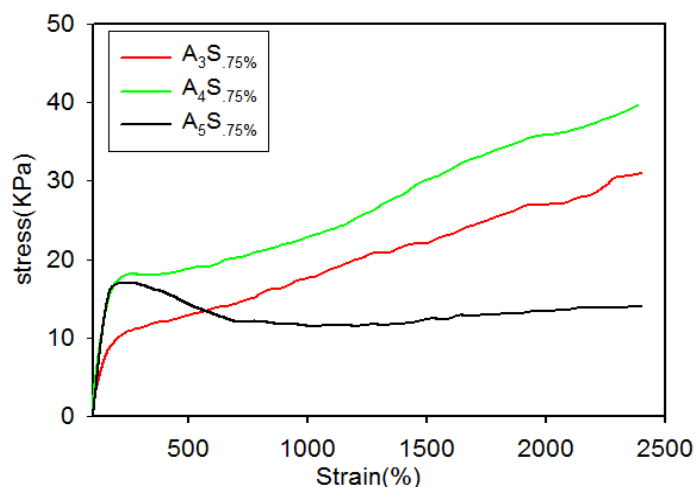


Fig. 3. 24: Stress –strain curves of AAm-MSiO₂ (117.5nm) hydrogels prepared by varying concentration of AAm under uniaxial tension.

Table 3. 14 :Table for tensile properties of AAm-MSiO₂ (117.5 nm) hydrogels prepared by varying concentration of AAm

Sample code	Toughness (kJ/m ³)	Tensile Strength (KPa)	Young Modulus (KPa)	Elongation at break (%)
A ₃ S _{.75%}	409	30	0.16	No break
A ₄ S _{.75%}	594	42	0.20	No break
A ₅ S _{.75%}	296	17	0.29	No break

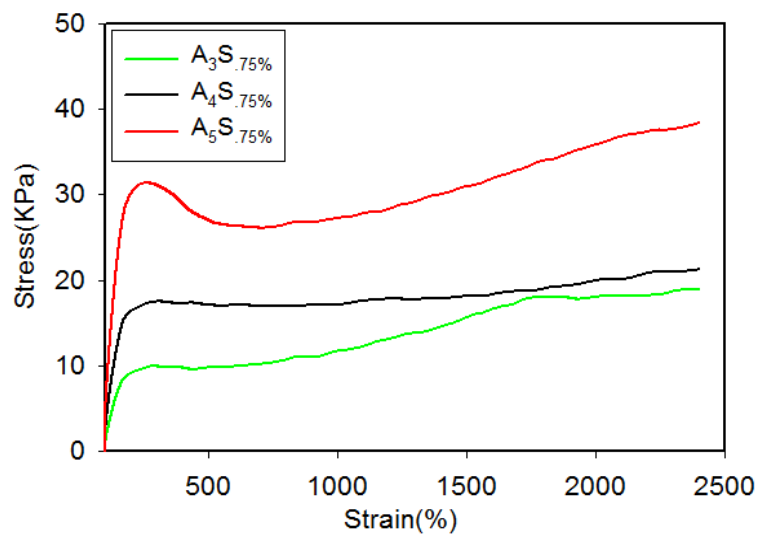


Fig. 3. 23: Stress –strain curves of AAm-MSiO₂ (216.5nm) hydrogels prepared by varying concentration of AAm under uniaxial tension.

Table 3. 15: Table for tensile properties of AAm-MSiO₂ (216.5nm) hydrogels prepared by varying concentration of AAm

Sample code	Toughness (kJ/m ³)	Tensile Strength (KPa)	Young Modulus (KPa)	Elongation at break (KPa)
A ₃ S _{.75%}	316	19	0.15	No break
A ₄ S _{.75%}	415	21	0.22	No break
A ₅ S _{.75%}	704	38	0.44	No break

The mechanical properties of hydrogels initially increase with increasing monomer concentration where crosslinker amount is fixed. However, above a threshold monomer concentration, the mechanical properties for each hydrogel reaches to a plateau value.

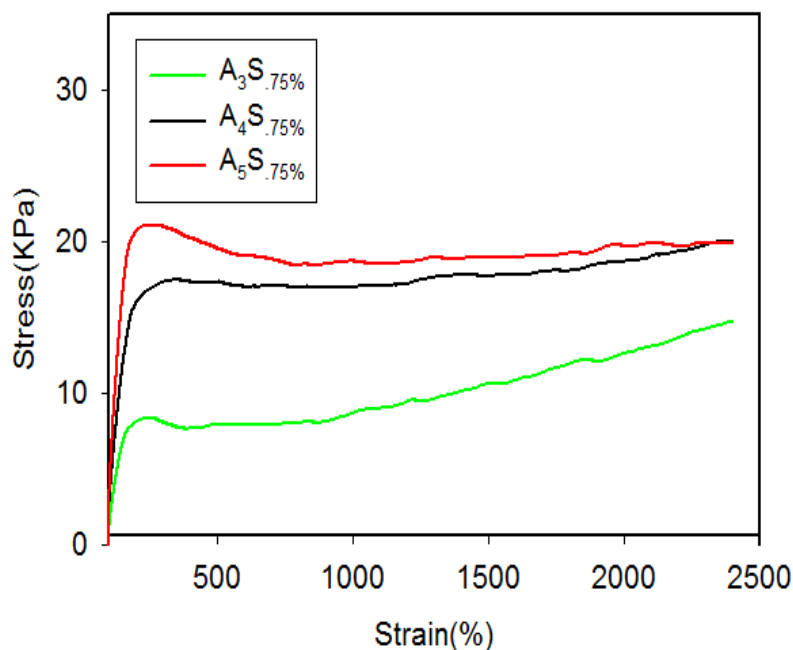


Fig. 3. 24 : Stress –strain curves of AAm-MSiO₂ (311.5nm) hydrogels prepared by varying concentration of AAm under uniaxial tension.

Table 3. 16: Table for tensile properties of AAm-MSiO₂ (311.5nm) hydrogels prepared by varying concentration of AAm

Sample code	Toughness (kJ/m ³)	Tensile Strength (KPa)	Young Modulus (KPa)	Elongation at break (%)
A ₃ S _{.75%}	231	11	0.11	No break
A ₄ S _{.75%}	403	20	0.17	No break
A ₅ S _{.75%}	440	21	0.25	No break

3.12.9 Compressive strength of AAm-MSiO₂ hydrogels (117.5 nm, 216.5 nm and 311.5 nm) prepared by varying concentration of AAm

The AAm concentration also has great effect on the compressive strength of AAm–

MSiO₂ hydrogel [7]. Figure 3.25, 3.26 and 3.27 shows that the toughness, compressive strength and Young's modulus of hydrogel significantly increases with increasing AAm concentration under the constant weight (%) of MSiO₂. AAm-MSiO₂ hydrogel with high AAm concentration possesses higher compressive strength due to strong bonding between the polymer chain and MSiO₂ particles and high entanglement of AAm polymer chains. Hence, when the AAm concentration is increased, the compressive strength, toughness and young modulus of hydrogel are increased (Table 3.17, Table 3.18 and Table 3.19).

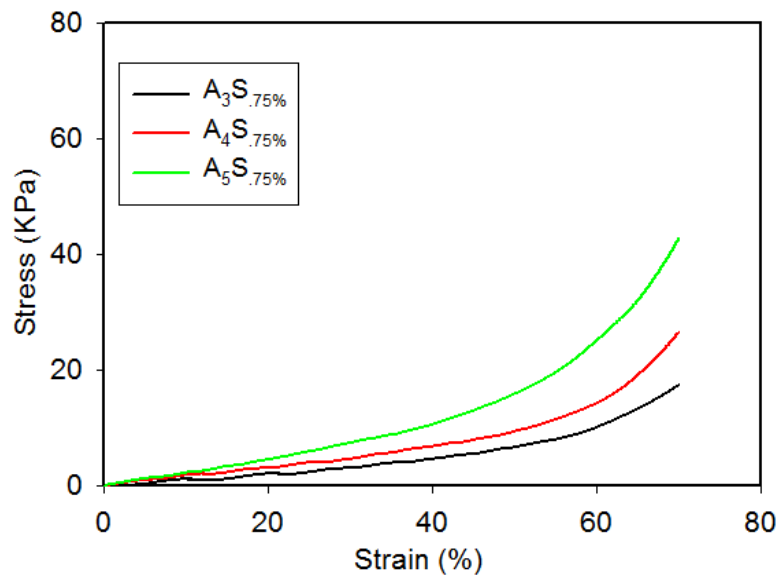


Fig. 3. 25 : Stress –strain curves of AAm-MSiO₂ (117.5nm) hydrogels prepared by varying concentration of AAm under uniaxial compression.

Table 3. 17: Table for compressive properties of AAm-MSiO₂ (117.5nm) hydrogels prepared by varying concentration of AAm

Concentration of AAm(M)	Toughness (kJ/m ³)	Compressive Strength (KPa)	Young Modulus (KPa)
A ₃ S _{.75%}	3.5	18	0.11
A ₄ S _{.75%}	5.2	26	0.15
A ₅ S _{.75%}	8.9	43	0.25

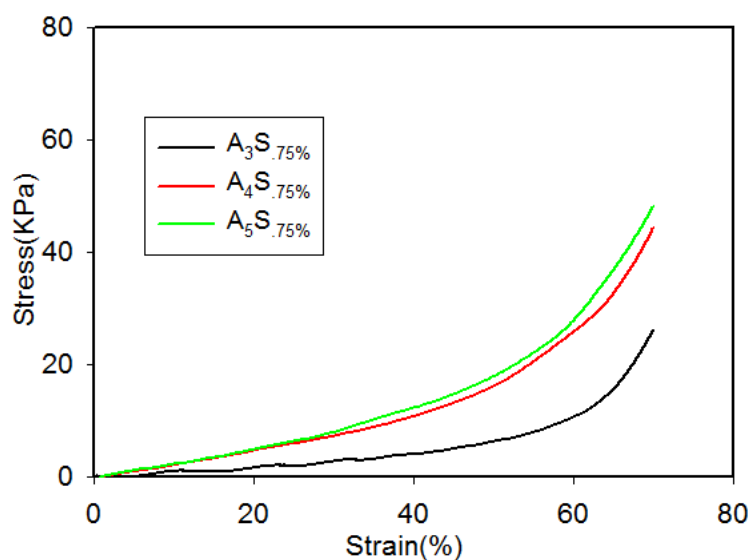


Fig. 3. 26 : Stress –strain curves of AAm-MSiO₂ (216.5 nm) hydrogels prepared by varying concentration of AAm under uniaxial compression.

Table 3. 18: Table for compressive properties of AAm-MSiO₂ (216.5 nm) hydrogels prepared by varying concentration of AAm

Sample code	Toughness (kJ/m ³)	Compressive Strength (KPa)	Young Modulus (KPa)
A ₃ S _{.75%}	4	26	0.10
A ₄ S _{.75%}	9	44	0.18
A ₅ S _{.75%}	10	49	0.27

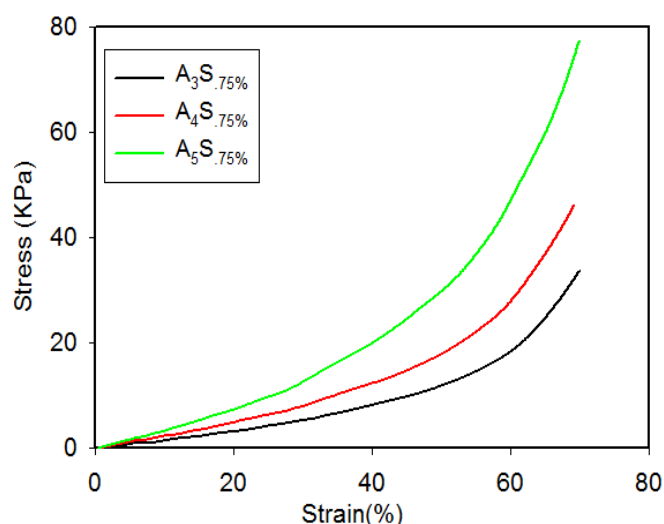


Fig. 3. 27 : Stress –strain curves of AAm-MSiO₂ (311.5 nm) hydrogels prepared by varying concentration of AAm under uniaxial compression.

Table 3. 19: Table for compressive properties of AAm-MSiO₂ (311.5 nm) hydrogels prepared by varying concentration of AAm

Sample code	Toughness (kJ/m ³)	Compressive Strength (KPa)	Young Modulus (KPa)
A ₃ S _{.75%}	6	34	0.19
A ₄ S _{.75%}	9	46	0.27
A ₅ S _{.75%}	16	78	0.41

3.12.10 Comparison of tensile test of AAm-MSiO₂ hydrogels prepared by varying particle sizes of MSiO₂ (117.5 nm, 216.5 nm, 311.5 nm)

The particles size has also determining factor for the mechanical properties of the hydrogel. The tensile properties of the hydrogel are increased with decreasing particle size. The smaller particle size carries the large surface area which are modified by more MPTS than the large particle size [8]. As a result, the smaller particle size crosslinker forms the more crosslinking point with the polymer chains to form high crosslinking density. Furthermore, the interaction between polymer chains and crosslinker also increases. As a result, it shows more restriction effect on the movement of the polymer

chain during elongation and shows higher tensile strength, young modulus and toughness. On the other hand, when the particle size of MSiO₂ crosslinker increases, less interaction between the polymer chain and crosslinker are effective. After maintain a constant concentration of AAm and MSiO₂ (%) and only by changing the size of silica particle from 100 nm to 300 nm; the tensile strength, toughness and elastic modulus of the hydrogel decreased from 30 KPa to 11 KPa, 409 kJ/m³ to 231kJ/m³ and 0.16 KPa to 0.11KPa, respectively. This trend has been continued for different concentration of AAm (fig 3.30 and fig 3.31). The mechanical properties also increase which is shown in the Table 3.20, Table 3.21 and Table 3.22.

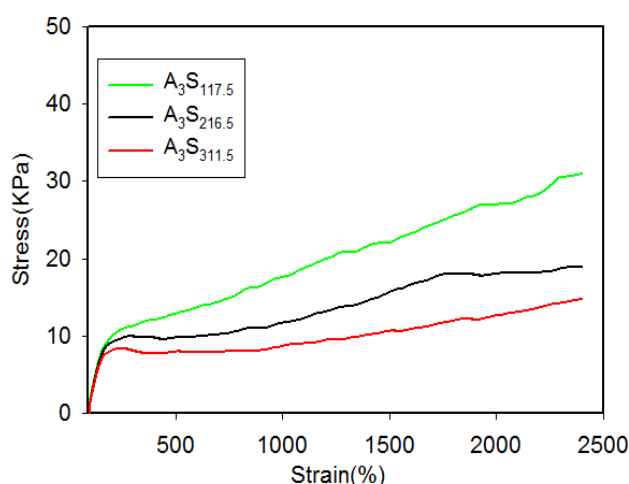


Fig. 3. 30 : Stress –strain curves of AAm-MSiO₂ hydrogels prepared by varying particle sizes of MSiO₂ (117.5 nm, 216.5 nm,311.5 nm) but AAm concentration kept constant as 3M under uniaxial tension.

Table 3. 20: Table for tensile properties of AAm-MSiO₂ hydrogels prepared by varying particle sizes of MSiO₂ (117.5 nm, 216.5 nm,311.5 nm) but AAm concentration kept constant as 3M

Sample Code	Toughness (kJ/m ³)	Tensile Strength (KPa)	Young Modulus (KPa)	Elongation at break (%)
A ₃ S _{117.5}	409	30	0.16	No break
A ₃ S _{216.5}	316	19	0.15	No break
A ₃ S _{311.5}	231	11.2	0.11	No break

When the concentration of AAm is increased from 3M to 4M, the tensile strength, toughness and Young’s modulus are also increased from 11.2 KPa to 19 KPa, 240.5kj/m³ to 436.9kj/m³ and 2.5KPa to 4kPa, respectively. The size of the MSiO₂ particle is same as 216.5nm. This trend is followed for the other sizes of MSiO₂ (Table 3.21 and Table 3.22).

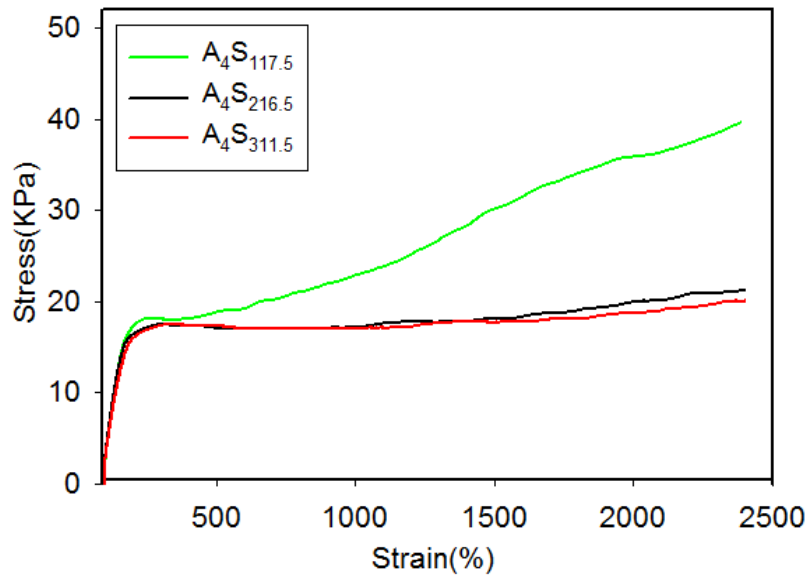


Fig. 3. 28 : Stress –strain curves of AAm-MSiO₂ hydrogels prepared by varying particle sizes of MSiO₂ (117.5 nm, 216.5 nm,311.5 nm) but AAm concentration kept constant as 4M under uniaxial tension.

Table 3. 21:Table for tensile properties of AAm-MSiO₂ hydrogels prepared by varying particle sizes of MSiO₂ (117.5 nm, 216.5 nm,311.5 nm) but AAm concentration kept constant as 4M

Sample code	Toughness (kJ/m ³)	Tensile Strength (KPa)	Young Modulus (KPa)	Elongation at break (%)
A ₄ S _{117.5}	594	42	0.20	No break
A ₄ S _{216.5}	415	21	0.22	No break
A ₄ S _{311.5}	403	20	0.17	No break

The mechanical properties for the 5M AAm-MSiO₂ hydrogel does not follow the same

trend as the 3M and 4M AAm-MSiO₂ hydrogel. There are two factors for this exceptional behavior, one is AAm concentration another is MSiO₂ particle size. Both are combined effect for showing the less mechanical properties than the other two hydrogels. The increasing particle size of MSiO₂ from 117.5 nm to 311.5 nm, the mechanical properties decrease for 3M, 4M and 5M AAm concentration except for the 5M, 117.5 nm sized MSiO₂ AAm-MSiO₂ hydrogel. In this specific particle size and concentration of AAm show the low mechanical properties due to the less amount of covalent bond with the polymer chains and presence of inhomogeneity in the network.

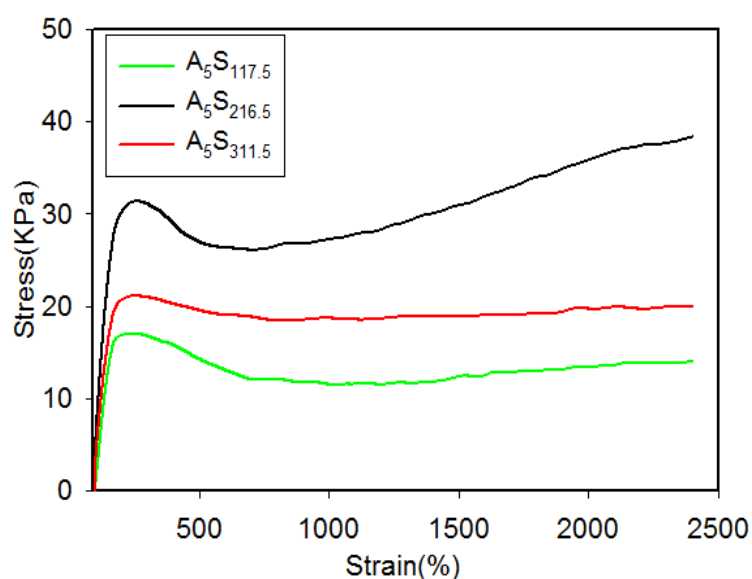


Fig. 3. 29 : Stress –strain curves of AAm-MSiO₂ hydrogels prepared by varying particle sizes of MSiO₂ (117.5 nm, 216.5 nm, 311.5 nm) but AAm concentration kept constant as 5M under uniaxial tension.

Table 3. 22: Table for tensile properties of AAm-MSiO₂ hydrogels prepared by varying particle sizes of MSiO₂ (117.5 nm, 216.5 nm, 311.5 nm) but AAm concentration kept constant as 5M

Sample code	Toughness (kJ/m ³)	Tensile Strength (KPa)	Young Modulus (KPa)	Elongation at break (%)
A ₅ S _{117.5}	296	17	0.29	No break
A ₅ S _{216.5}	704	38	0.44	No break
A ₅ S _{311.5}	440	21	0.25	No break

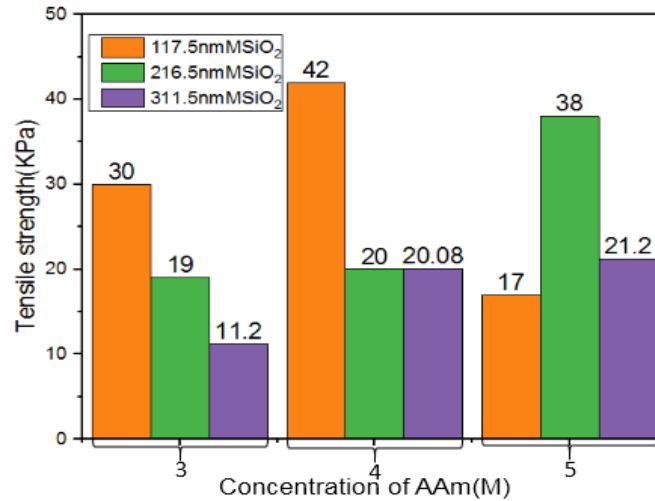


Fig. 3. 30 :Tensile strength of AAm-MSiO₂ hydrogel with different concentration of AAm for elongation

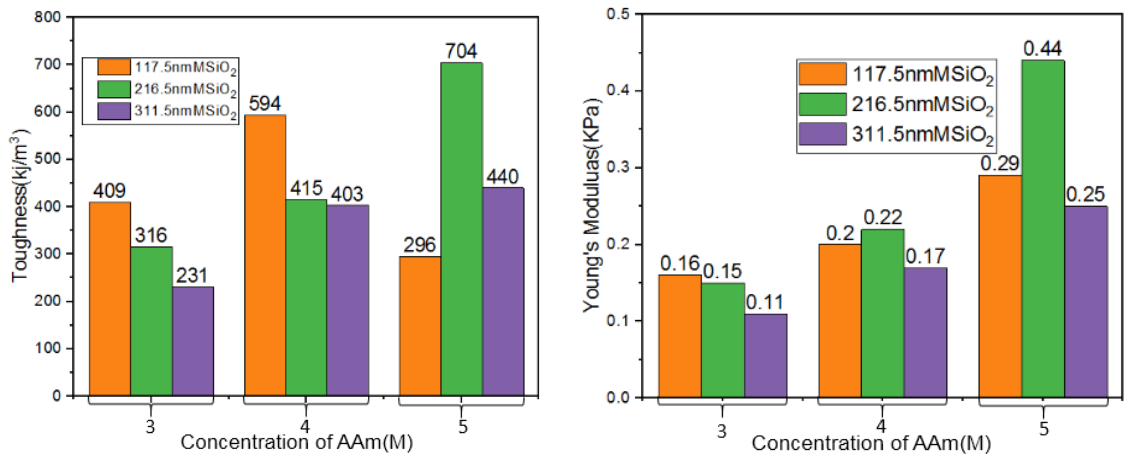


Fig. 3. 31 :Toughness and young’s modulus of AAm-MSiO₂ hydrogel with different concentration of AAm for elongation

3.12.11 Comparison of compressive strength of AAm-MSiO₂ hydrogels prepared by varying particle sizes of MSiO₂ (117.5 nm, 216.5 nm,311.5 nm)

The stress-strain curves for compressive strength of AAm-MSiO₂ hydrogels prepared by varying particle sizes of MSiO₂ (117.5 nm, 216.5 nm,311.5 nm) and different concentration of AAm are shown in Fig. 3.32, Fig. 3.33 and Fig. 3.34. When a stress is applied on the hydrogel, the total energy can be dissipated throughout the homogeneously distributed hydrogel network. Table 3.23, Table 3.24 and Table 3.25. shows the compressive strength, Young’s modulus and toughness of AAm-MSiO₂ hydrogels using constant 0.75% of MSiO₂. The increasing particle size of MSiO₂, the

compressive strength, toughness as well as young's modulus of AAm-MSiO₂ hydrogels are increased. When the particle size of MSiO₂ increases, AAm-MSiO₂ hydrogels crosslinked with bigger crosslinker presented higher elastic and compressive modulus, relative to those crosslinked using crosslinkers of small particle size [9]. We hypothesize that bigger crosslinks lead to an increase in the ordered structure of the hydrogel network. And another view that the bigger particles are generally much harder and rigid than the small particles. When a force is applied to the hydrogels which contained different MSiO₂ size particles as crosslinker, the larger particle size containing hydrogels restricted more the applied force than the small size containing hydrogels. As a result, the hydrogels are capable of resisting a great compressive force and shows higher compressive strength, toughness and Young's modulus.

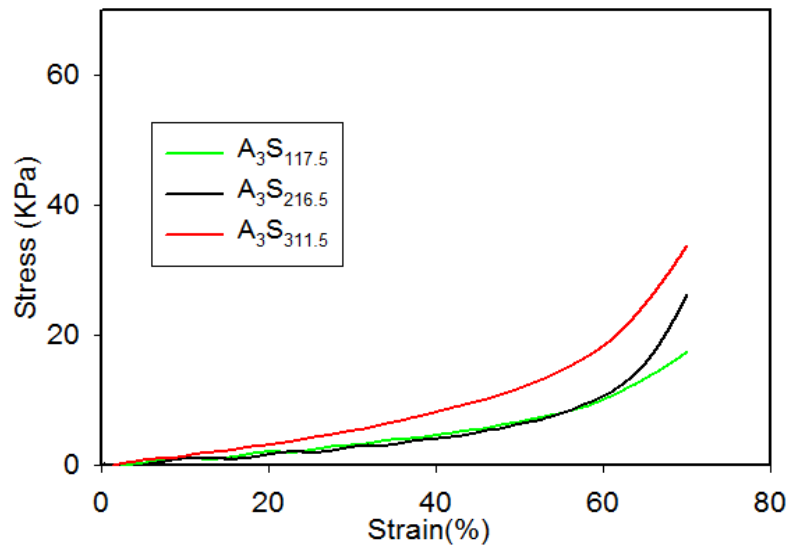


Fig. 3. 32 : Stress –strain curves of AAm-MSiO₂ hydrogels prepared by varying particle sizes of MSiO₂ (117.5 nm, 216.5 nm,311.5 nm) but AAm concentration kept constant as 3M under uniaxial compression.

Table 3. 23: Table for compressive properties of AAm-MSiO₂ hydrogels prepared by varying particle sizes of MSiO₂ (117.5nm, 216.5nm,311.5nm) but AAm concentration kept constant as 3M

Sample code	Toughness (kJ/m ³)	Compressive Strength (KPa)	Young Modulus (KPa)
A ₃ S _{117.5}	6	34	0.11
A ₃ S _{216.5}	4	26	0.10
A ₃ S _{311.5}	4	18	0.19

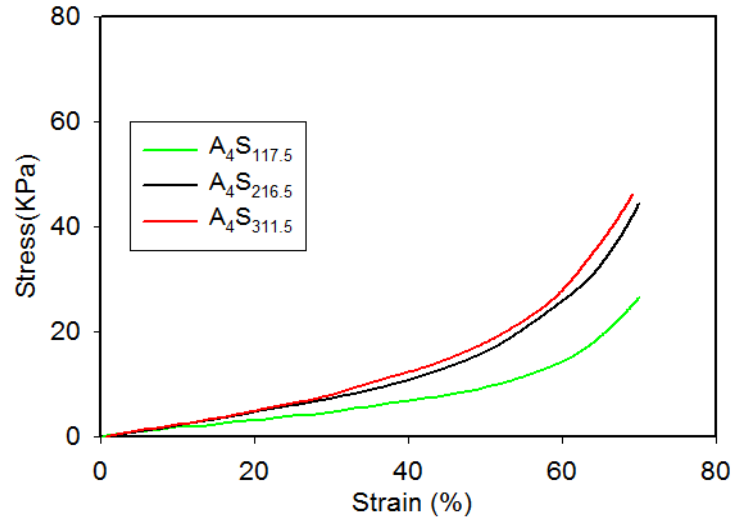


Fig. 3. 33 : Stress –strain curves of AAm-MSiO₂ hydrogels prepared by varying particle sizes of MSiO₂ (117.5 nm, 216.5 nm,311.5 nm) but AAm concentration kept constant as 4M under uniaxial compression.

Table 3. 24 :Table for compressive properties of AAm-MSiO₂ hydrogels prepared by varying particle sizes of MSiO₂ (117.5 nm, 216.5 nm,311.5 nm) but AAm concentration kept constant as 4M

Sample code	Toughness (kJ/m ³)	Compressive Strength (KPa)	Young Modulus (KPa)
A ₄ S _{117.5}	5	44	0.15
A ₄ S _{216.5}	9	39	0.26
A ₄ S _{311.5}	9	26	0.27

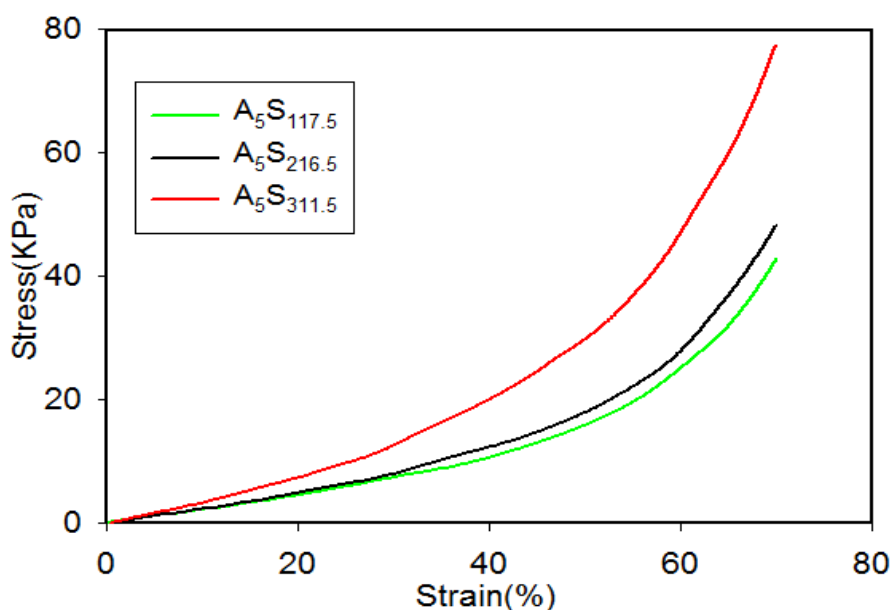


Fig. 3. 34 : Stress –strain curves of AAm-MSiO₂ hydrogels prepared by varying particle sizes of MSiO₂ (117.5 nm, 216.5 nm,311.5 nm) but AAm concentration kept constant as 5M under uniaxial compression.

Table 3. 25 : Table for compressive properties of AAm-MSiO₂ hydrogels prepared by varying particle sizes of MSiO₂ (117.5 nm, 216.5 nm,311.5 nm) but AAm concentration kept constant as 5M

Sample code	Toughness (kJ/m ³)	Compressive Strength (KPa)	Young Modulus (KPa)
A ₅ S _{117.5}	5	26	0.15
A ₅ S _{216.5}	10	49	0.27
A ₅ S _{311.5}	16	78	0.41

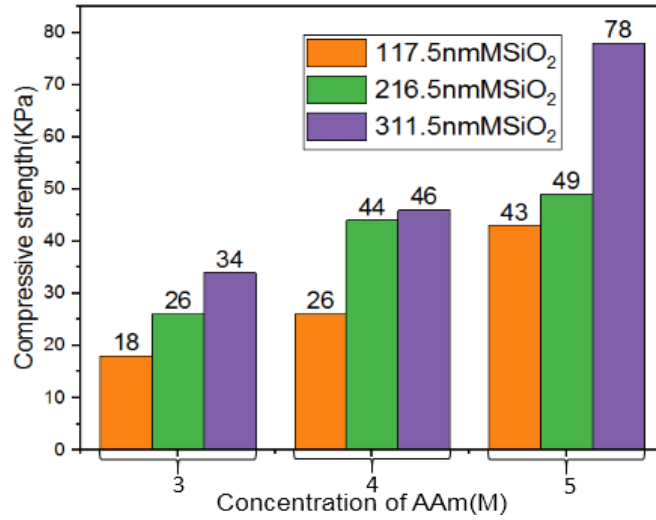


Fig. 3. 35: Compressive strength of AAm-MSiO₂ hydrogel with different concentration of AAm

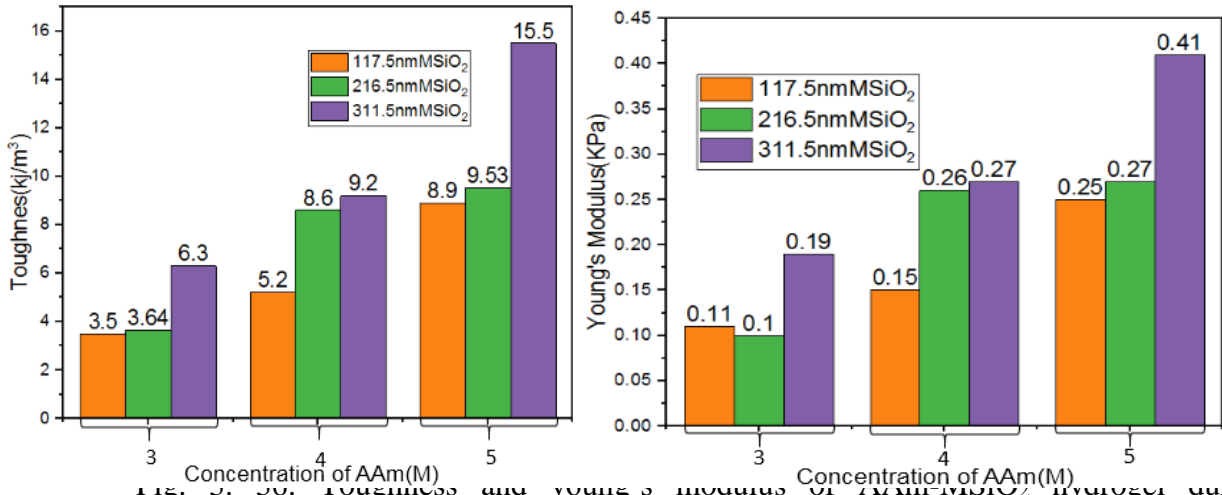


Fig. 3. 36: Toughness and young's modulus of AAm-MSiO₂ hydrogel during compression in different concentration of AAm

3.13 Photographs of AAm-MSiO₂ hydrogel during analysis of stress-strain curves under uniaxial tensile deformation

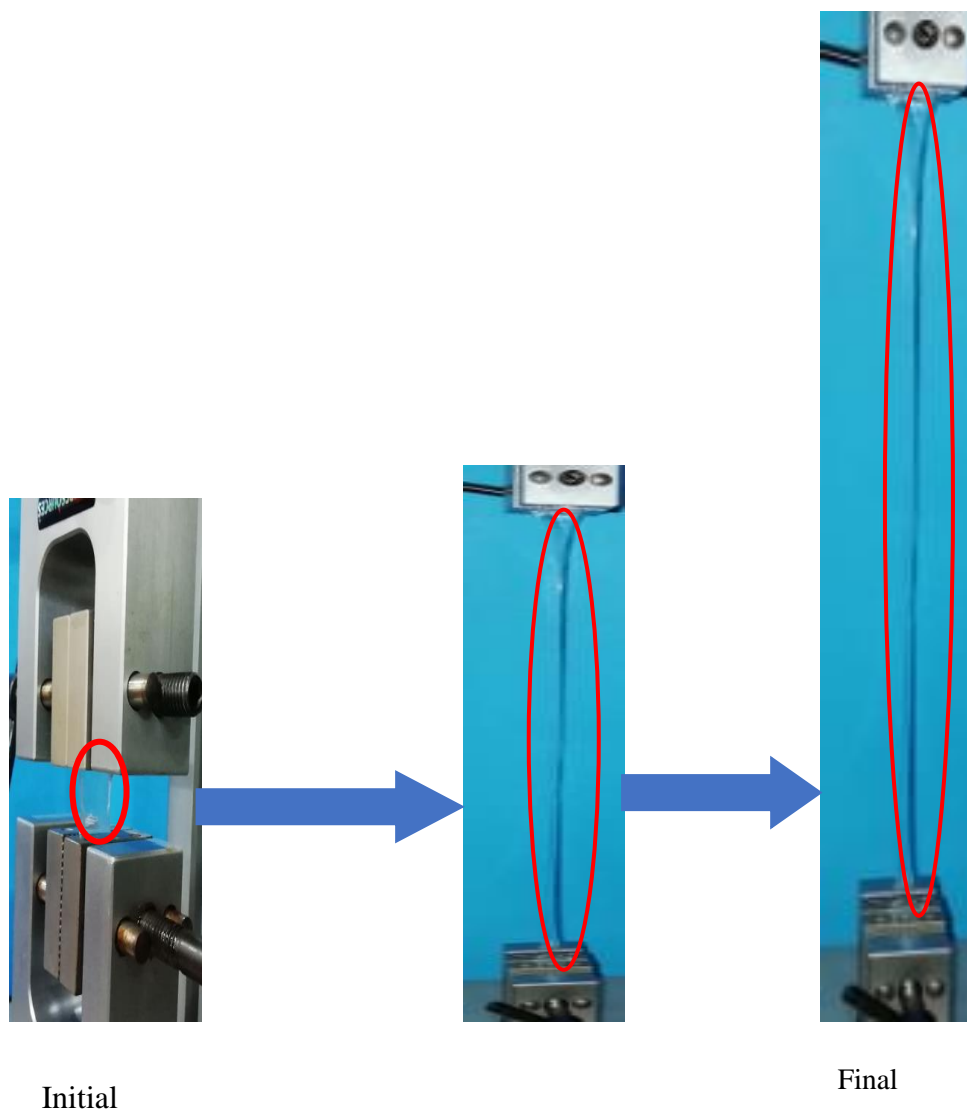


Fig. 3. 37: Photographs of AAm-MSiO₂ hydrogel during analysis of stress-strain curves under uniaxial tension

3.14: Photographs of AAm-MSiO₂ hydrogel during analysis of stress-strain curves under uniaxial compressive deformation

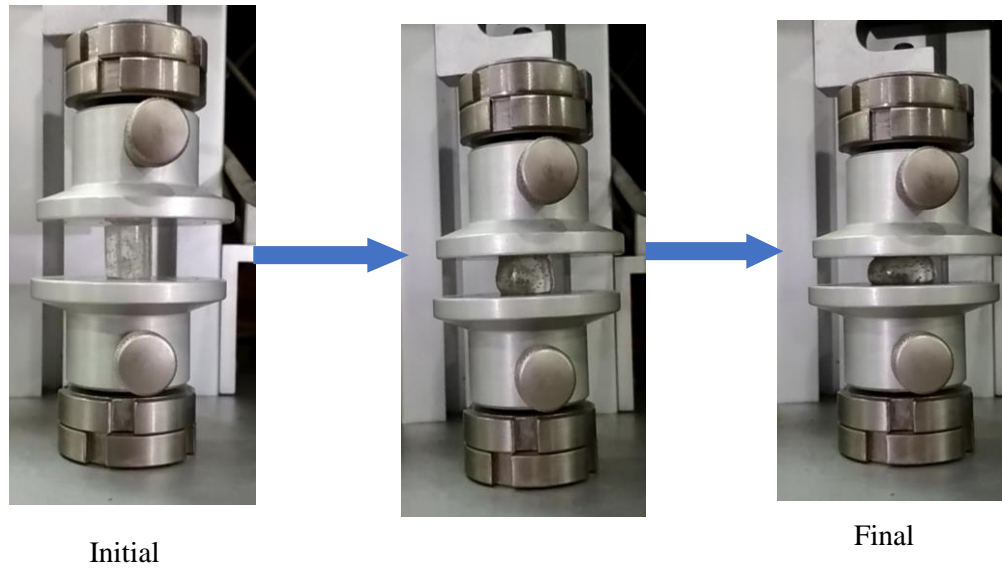


Fig. 3. 38: Photographs of AAm-MSiO₂ hydrogel during analysis of stress-strain curves under uniaxial compressive deformations

3.15. References

- [1] K. Haraguchi, "Nanocomposite hydrogels," *Current Opinion in Solid State and Materials Science*, vol.11, pp. 47-54 (2007).
- [2] R. Liu, S. Liang, X. Z. Tang, D. Yan, X. Li, and Z. Z. Yu, "Tough and highly stretchable graphene oxide/polyacrylamide nanocomposite hydrogels," *J. Mater. Chem.*, vol. 22, pp. 14160-14167 (2012).
- [3] T. L. Wang, C. C. Ou, and C. H. Yang, "Synthesis and properties of organic/inorganic hybrid nanoparticles prepared using atom transfer radical polymerization," *J. Appl. Polym. Sci.*, vol. 109, pp.3421-3430 (2008).
- [4] M. O. Haque and M. I. H. Mondal, "Synthesis and Characterization of Cellulose-based Eco-Friendly Hydrogels," *Rajshahi Univ. J. Sci. Eng.*, vol.44, pp. 45-53 (2016).
- [5] J. A. Burdick, "Injectable gels for tissue/organ repair," *Biomed. Mater.*, vol.7, pp. 1-2 (2012).
- [6] N. Zhou *et al.*, "Degradation prediction model and stem cell growth of gelatin-PEG composite hydrogel," *J. Biomed. Mater. Res. - Part A*, vol. 104, pp. 3149-3156 (2016).
- [7] Y. Hagiwara, A. Putra, A. Kakugo, H. Furukawa, and J. P. Gong, "Ligament-like tough double-network hydrogel based on bacterial cellulose," *Cellulose*, vol.17, pp.93-101 (2010).
- [8] J. Yang, J. J. Zhao, C. R. Han, and J. F. Duan, "Keys to enhancing mechanical properties of silica nanoparticle composites hydrogels: The role of network structure and interfacial interactions," *Compos. Sci. Technol.*, vol. 95, pp. 1–7, (2014).
- [9] D. Yang *et al.*, "Fabrication of a highly elastic nanocomposite hydrogel by surface modification of cellulose nanocrystals," *RSC Adv.*, vol.5, pp.13878-13885 (2015).

Chapter 4

Conclusion

4. Conclusion

Vinyl containing modified silica (MSiO_2) particle is successfully synthesized by reacting narrow dispersed silica particles (SiO_2) with a silane coupling agent, 3-Methacryloxypropyltrimethoxysilane (MPTS) which is confirmed by FESEM, EDS, FT-IR $^1\text{H-NMR}$ analysis. Poly(acrylamide) hydrogel is prepared successfully by cross-linked with MSiO_2 cross-linker by the formation of covalent bonds between the MSiO_2 and AAm polymer chain through *in-situ* free-radical polymerization. These synthesized nanocomposite hydrogels are highly transparent which confirm the homogeneous network formation in the hydrogels. The AAm- MSiO_2 cross-linked hydrogel shows the excellent toughness and elongation at break than the conventional N,N'-methylenebisacrylamide (BIS) crosslinker containing hydrogel. Here, all AAm- MSiO_2 hydrogels are elongated 2400% from their initial state without any break but AAm-BIS hydrogels are elongated only to a maximum 160%. Among the AAm- MSiO_2 hydrogels, the tensile strength, toughness, and Young's modulus are increased in a plateau with the increase of cross-linker and AAm monomer amount. The tensile strength, toughness, Young's modulus is decreased with the increase of MSiO_2 size from 117.5nm to 311.5 nm under uniaxial tensile deformation. The hydrogel prepared by MSiO_2 (117.5 nm) exhibits highest tensile strength, toughness and Young's modulus during elongation compare with other hydrogels. In contrasts, AAm- MSiO_2 hydrogel having the large MSiO_2 particle size shows higher compressive strength, toughness and Young modulus compare with other hydrogels under uniaxial compressive deformation.

Publication, Attended conference and Achievement

Publications:

1. Md. Rezaul Karim and Abu Bin Imran Fabrication of highly stretchable hydrogel using narrow dispersed modified nanosilica particles as cross-linker (in preparation)
2. Md. Rezaul Karim and Abu Bin Imran Effect of particle sizes of nanosilica cross-linker on the mechanical properties of acrylamide-modified silica based nanocomposite hydrogel (in preparation)

Conference:

1. Md. Rezaul Karim and Abu Bin Imran . Mechanical properties enhancement of hydrogel using narrow disperse modified silica particles as cross-linker, 5th Conference of Bangladesh Crystallographic Association, Bangladesh Crystallographic Association , University of Dhaka, Dhaka. 25-26 January, 2019

Achievement:

1. Best poster award for the presentation on Mechanical properties enhancement of hydrogel using narrow disperse modified silica particles as cross-linker in 5th Conference of Bangladesh Crystallographic Association, Bangladesh Crystallographic Association , University of Dhaka, Dhaka. 25-26 January, 2019